

Ionic Currents and Spontaneous Firing in Neurons Isolated from the Cerebellar Nuclei

Indira M. Raman,^{1,2} Amy E. Gustafson,² and Daniel Padgett²

¹Department of Neurobiology and Physiology and ²Integrated Science Program, Northwestern University, Evanston, Illinois 60208

Neurons of the cerebellar nuclei fire spontaneous action potentials both *in vitro*, with synaptic transmission blocked, and *in vivo*, in resting animals, despite ongoing inhibition from spontaneously active Purkinje neurons. We have studied the intrinsic currents of cerebellar nuclear neurons isolated from the mouse, with an interest in understanding how these currents generate spontaneous activity in the absence of synaptic input as well as how they allow firing to continue during basal levels of inhibition. Current-clamped isolated neurons fired regularly (~20 Hz), with shallow interspike hyperpolarizations (approximately –60 mV), much like neurons in more intact preparations. The spontaneous firing frequency lay in the middle of the dynamic range of the neurons and could be modulated up or down with small current injections.

During step or action potential waveform voltage-clamp commands, the primary current active at interspike potentials was a

tetrodotoxin-insensitive (TTX), cesium-insensitive, voltage-independent, cationic flux carried mainly by sodium ions. Although small, this cation current could depolarize neurons above threshold voltages. Voltage- and current-clamp recordings suggested a high level of inactivation of the TTX-sensitive transient sodium currents that supported action potentials. Blocking calcium currents terminated firing by preventing repolarization to normal interspike potentials, suggesting a significant role for K(Ca) currents. Potassium currents that flowed during action potential waveform voltage commands had high activation thresholds and were sensitive to 1 mM TEA. We propose that, after the decay of high-threshold potassium currents, the tonic cation current contributes strongly to the depolarization of neurons above threshold, thus maintaining the cycle of firing.

Key words: deep cerebellar nuclei; pacemaking; action potential; sodium channel; cation channel; persistent sodium current

Many neurons fire regular, spontaneous, sodium-dependent action potentials, even in the absence of synaptic input (Llinás and Sugimori, 1980; Williams et al., 1984; Jahnsen, 1986a; Grace and Onn, 1989; Yung et al., 1991; du Lac and Lisberger, 1995; Mougnot and Gähwiler, 1995; Uteshev et al., 1995; Bayliss et al., 1997). Spontaneous firing can be generated in several ways. In some neurons, low-threshold calcium currents and hyperpolarization-activated cation currents (I_h ; Mayer and Westbrook, 1983) are recruited by afterhyperpolarizations and depolarize the membrane before each action potential (McCormick and Pape, 1990). In neurons with less prominent afterhyperpolarizations, spontaneous firing might occur if the currents that determine the resting potential (if spikes could be prevented) equilibrate at potentials sufficiently positive for significant activation of transient sodium currents. In some cells these steady “resting” currents are carried by tetrodotoxin-sensitive (TTX) sodium channels (Pennartz et al., 1997; Feigenspan et al., 1998; Bevan and Wilson, 1999; Raman and Bean, 1999) or I_h channels (Ghamari-Langroudi and Bourque, 2000). Other potential candidates for such currents include voltage-gated calcium currents and nonspecific cation currents.

Steady currents that depolarize the cell to suprathreshold voltages might not guarantee spontaneous activity, however. If the resting potential were set at too depolarized a level or if depolarization were to occur too slowly, then transient sodium currents might inactivate to such an extent that spontaneous firing would not persist. Additionally, firing might fail to occur if small depolarizations were to recruit large opposing currents, such as low-threshold potassium currents.

Neurons of the cerebellar nuclei are spontaneously active in semi-intact preparations and fire regularly in resting animals *in vivo* (Thach, 1968; Jahnsen, 1986a; McDevitt et al., 1987; Llinás and Mühlethaler, 1988; Mougnot and Gähwiler, 1995; Czubyko et al., 1998; Aizenman and Linden, 1999). To our knowledge, however, no voltage-clamp studies have been published of the intrinsic currents that produce the firing patterns of these neurons. The spontaneous activity of cerebellar nuclear neurons is particularly interesting because they are the primary targets of Purkinje neurons, which not only are inhibitory (Ito et al., 1970), but themselves fire spontaneous high-frequency action potentials (~50 Hz; Häusser and Clark, 1997; Nam and Hockberger, 1997; Raman and Bean, 1997). Thus the observed spontaneous firing of cerebellar nuclear neurons apparently persists even during what must be a considerable barrage of inhibition.

To characterize the intrinsic ionic currents of these cells, we recorded voltage-clamped ionic currents and action potentials of large neurons isolated from cerebellar nuclei of mice. Our results suggest that firing persists despite a low availability of TTX-sensitive sodium current and that small hyperpolarizations can recruit a substantial proportion of sodium channels. Neither TTX-sensitive persistent sodium current nor voltage-gated calcium currents nor I_h appears to be necessary to depolarize the neurons above threshold voltages. Instead, a tonic, voltage-independent, TTX-insensitive cation current, carried mainly by sodium ions, dominates the interspike interval. This small but potent cation current, transient TTX-sensitive currents, and high-threshold TEA-sensitive potassium currents appear to interact to allow regular firing to persist in isolated cerebellar nuclear neurons.

MATERIALS AND METHODS

Preparation of isolated neurons. Neurons from the cerebellar nuclei were isolated from 10- to 17-d-old pigmented mice, either Black Swiss (Taconic Farms, Germantown, NY) or C57BL6 (Charles River, Wilmington, MA). Control experiments were performed on neurons from the ventral cochlear nucleus from age-matched mice. Cells were dissociated according to techniques adapted from Raman and Trussell (1992). Animals were anesthetized with methoxyflurane and decapitated. On a vibroslicer, parasagittal

Received July 28, 2000; revised Sept. 26, 2000; accepted Sept. 27, 2000.

This work was supported by National Institutes of Health Grant NS39395 (I.M.R.). I.M.R. is a fellow of the Alfred P. Sloan Foundation and the Searle Foundation. We thank Dr. Nace Golding for his help in dissecting the ventral cochlear nucleus and Drs. Larry Trussell and Nelson Spruston for comments on this manuscript.

Correspondence should be addressed to Dr. Indira M. Raman, Department of Neurobiology and Physiology, Northwestern University, 2153 North Campus Drive, Evanston, IL 60208. E-mail: i-raman@nwu.edu.

Copyright © 2000 Society for Neuroscience 0270-6474/00/209004-13\$15.00/0

cerebellar slices (or cochlear nuclear slices) were cut in control Tyrode's solution, which contained (in mM) 150 NaCl, 4 KCl, 2 CaCl₂, 2 MgCl₂, 10 HEPES, and 10 glucose, pH 7.4 (adjusted with NaOH; final sodium concentration of 155 mM). The slices were incubated for 20 min at 31°C in MEM (Life Technologies, Gaithersburg, MD) with (in mM) 10 HEPES, 1 cysteine, and 0.5 EDTA, pH 7.2, to which 40 U/ml papain (Worthington, Lakewood, NJ) had been added. After enzymatic treatment the slices were washed in MEM-HEPES to which 1 mg/ml trypsin inhibitor and 1 mg/ml bovine serum albumin had been added. Under the dissecting microscope the cerebellar nuclei were visible as the cell body-rich regions at the core of several slices. Cerebellar nuclei were dissected out of the slices with fine tungsten needles, and the tissue chunks were triturated with a series of fire-polished Pasteur pipettes to liberate both "large" and "small" cerebellar nuclear neurons. The large cells (15–25 μ m in soma diameter) are likely to be the glutamatergic neurons that project to the red nucleus and ventral thalamus (Bentivoglio and Kuypers, 1982; Gonzalo-Ruiz et al., 1988; Teune et al., 1995, 1998; Shinoda et al., 1997). The small cells (5–10 μ m in soma diameter) are likely to be inhibitory neurons that project to the inferior olive (Nelson and Mugnaini, 1989; Fredette and Mugnaini, 1991; Ruigrok, 1997). All cerebellar nuclear recordings were made from large neurons. For the ventral cochlear nucleus the entire nucleus was dissected from the brainstem, minced, and triturated. Bushy cells (~15 μ m diameter) were identified by their characteristic tear-shaped cell body and short dendritic tuft (Cant and Morest, 1979). The morphology of each cell was archived with a Scion Image frame grabber system (Research Biochemicals, Natick, MA).

Electrophysiological recordings. Current-clamp recordings were made with a BVC700 amplifier (Dagan, Minneapolis, MN). Voltage-clamp recordings were made with an Axopatch 200B amplifier (Axon Instruments, Foster City, CA), and series resistance was compensated by ~90%. Voltage steps as well as waveforms of prerecorded trains of action potentials were used as command waveforms (Llinás et al., 1982; McCobb and Bean, 1991; Raman and Bean, 1997, 1999). Data were recorded with an Instrutech ITC-18 interface (Great Neck, NY) and analyzed with PULSE and IGOR software.

Borosilicate pipettes (1–3 M Ω for voltage-clamp experiments; 4–6 M Ω for current-clamp experiments) were wrapped with Parafilm to minimize the pipette capacitance. Pipette as well as cell capacitance was neutralized further by using the amplifier circuitry. Pipettes were filled with one of two intracellular solutions. A physiological intracellular solution contained (in mM) 122 KCH₃O₂S, 9 EGTA, 9 HEPES, 1.8 MgCl₂, 15 sucrose, 14 Tris-creatine PO₄, 4 Mg-ATP, and 0.3 Tris-GTP buffered to pH 7.4 with KOH, for a final K⁺ concentration of 154 mM. This internal solution was used for all recordings, except as noted. In a few experiments, 5 mM KCl substituted for 5 mM KCH₃O₂S. This more physiological chloride concentration had no detectable effects on firing rate or current kinetics. A CsCl-based solution contained (in mM) 117 CsCl, 9 EGTA, 9 HEPES, 1.8 MgCl₂, 14 Tris-creatine PO₄, 4 Mg-ATP, and 0.3 Tris-GTP, buffered to pH 7.4 with CsOH. This solution was used for step command voltage-clamp experiments that involved pharmacological isolation of TTX-sensitive sodium currents (see Figs. 3, 5*A,B*).

The control physiological extracellular saline for action potential recordings and most voltage-clamp recordings was control Tyrode's solution. For experiments that required the blockade of calcium channels, Co Tyrode's solution was used, in which 2 mM CoCl₂ replaced 2 mM CaCl₂. For the experiments requiring low external sodium (see Figs. 10, 11), NMDG-Tyrode's solution was used, in which 150 mM *N*-methyl-D-glucamine-Cl replaced 150 mM NaCl. The NMDG-Tyrode's was buffered with NaOH, for a final sodium concentration of 6 mM. NMDG-Tyrode's and control Tyrode's had the same osmolarity, and there was no junction potential between them. Other blockers, such as TTX (900 nM), TEA (1 mM), or CsCl (2 mM), were added to Ca, Co, or NMDG-Tyrode's as needed. The IC₅₀ for TTX blockade of transient voltage-gated sodium currents was ~10 nM (data not shown). We therefore used 900 nM TTX in all experiments requiring blockade of both transient and persistent voltage-gated sodium currents, and we use the phrase "TTX-sensitive sodium currents" to refer to currents blocked by 900 nM TTX.

For voltage-clamp measurements of TTX-sensitive sodium currents evoked by voltage steps (see Figs. 3, 5*A,B*), the external solution (50 mM NaCl) contained (in mM) 50 NaCl, 110 TEA-Cl, 10 HEPES, and 2 CoCl₂, buffered to pH 7.4 with NaOH.

The different external solutions were applied through gravity-driven flow pipes, and the solution bathing the cell was controlled by positioning the cell in front of the desired pipe. Thus, an experimental protocol could be performed in a control solution and repeated in a solution containing a toxin or blocking agent; for voltage-clamp experiments, subtraction of the records gave the current sensitive to the blocker. The quality of the voltage clamp was considered adequate if the current-voltage relation for TTX-sensitive currents, measured with 2 mV increments, was smooth and if no outward current was evident in the TTX-subtracted records (Raman and Bean, 1999).

Voltage-current relations were measured in current clamp with 400 msec current injections given in 10 pA increments, usually from -100 to 100 pA. For steps that did not elicit action potentials and that brought the membrane potential between -70 and -120 mV, the mean voltage was measured between 290 and 390 msec after the current step. Input resis-

tances were estimated from linear fits to the plots of mean voltage against current.

All recorded voltages were corrected for junction potentials measured for each internal solution. Recordings were made at room temperature. All chemicals were obtained from Sigma (St. Louis, MO) except muscarine and ACPD, obtained from Research Biochemicals (Natick, MA). Data are reported as mean \pm SE. Statistical comparisons were made with Student's paired *t* tests, except as noted, and *p* values are reported.

RESULTS

Isolated cerebellar nuclear cells had a variety of morphologies but generally could be classified by size and dendritic structure. Large neurons tended to have cell bodies that were 15–25 μ m in diameter (Fig. 1*A*). Many had three or four primary dendrites, resembling the "large multipolar neurons" of Chan-Palay (1977). Other isolated large neurons resembled the "large cascade neurons" and "large columnar neurons" (Chan-Palay, 1977), the dendrites of which tend to be oriented in a single direction. Small neurons (5–10 μ m in soma diameter) also were released by the cell isolation procedure. These neurons are likely to be the inhibitory neurons that project to the inferior olive (Nelson and Mugnaini, 1989; Fredette and Mugnaini, 1991; Ruigrok, 1997). As described in Materials and Methods, the present experiments were limited to the large cerebellar nuclear neurons, which had similar electrophysiological properties.

Action potentials of isolated cerebellar nuclear neurons

Our first interest was to compare the firing properties of isolated cerebellar nuclear cells with those of neurons in more intact preparations. Under whole-cell current clamp in normal physiological saline, the majority of neurons fired regular trains of action potentials in the absence of current injection (50 of 57 cells). This spontaneous firing also was observed in the cell-attached patch configuration. Figure 1*B* illustrates spontaneous action potentials recorded from each cerebellar nuclear neuron in Figure 1*A*. The mean firing frequency of spontaneously active neurons was 18.3 ± 1.7 Hz ($n = 50$; Fig. 1*C*). Action potentials reached peaks of 23 ± 1.3 mV and had only moderately hyperpolarized troughs of -59 ± 0.7 mV ($n = 50$). The spontaneous firing rates and action potential waveforms were similar to those in semi-intact preparations. Specifically, mean firing rates near 20 Hz, as well as interspike trough potentials 20–30 mV positive to E_K , have been reported in acute slices, slice cultures, and brainstem–cerebellar preparations (Jahnsen, 1986*a,b*; Llinás and Mühlethaler, 1988; Mougnot and Gähwiler, 1995; Aizenman and Linden, 1999). These similarities suggest that the basic pacemaking mechanism may be conserved in the isolated cell preparation, although specific differences in the firing properties of isolated and intact cells are discussed below.

Spontaneously active neurons continued to fire during injection of small hyperpolarizing currents up to ~50 pA, as shown in Figure 2*A*. In slice studies, quantitatively similar results have been obtained with patch electrodes (Czubayko et al., 1998) and qualitatively similar results with microelectrodes (Aizenman and Linden, 1999). The frequency–intensity relations were linear, with slopes of 0.4 ± 0.06 Hz/pA and correlation coefficients ranging from 0.83 to 0.9997 ($n = 19$; Fig. 2*A*).

In response to small depolarizing current steps, the cells increased their firing rates (Fig. 2*B*, middle trace), although the amplitude of successive spikes often decreased during a step. Thirteen of 35 cells continued to fire with current injections up to 200 pA. In the other 22 cells, depolarizing current steps often led to a few action potentials in rapid succession, followed by cessation of firing (Fig. 2*B*, top trace). The current amplitude that produced this depolarization block averaged 87 ± 12 pA. During block, the membrane potential settled at -28.8 ± 1.5 mV. On termination of the step many cells remained at this plateau potential until the membrane was actively hyperpolarized by current injection (data not shown). In general, the isolated neurons seemed more disposed to depolarization block than neurons in slices, which have been reported to fire at a few hundred Hertz in response to current injection before settling at plateau potentials (Jahnsen, 1986*a*; Aizenman and Linden, 1999). This difference may be attributable

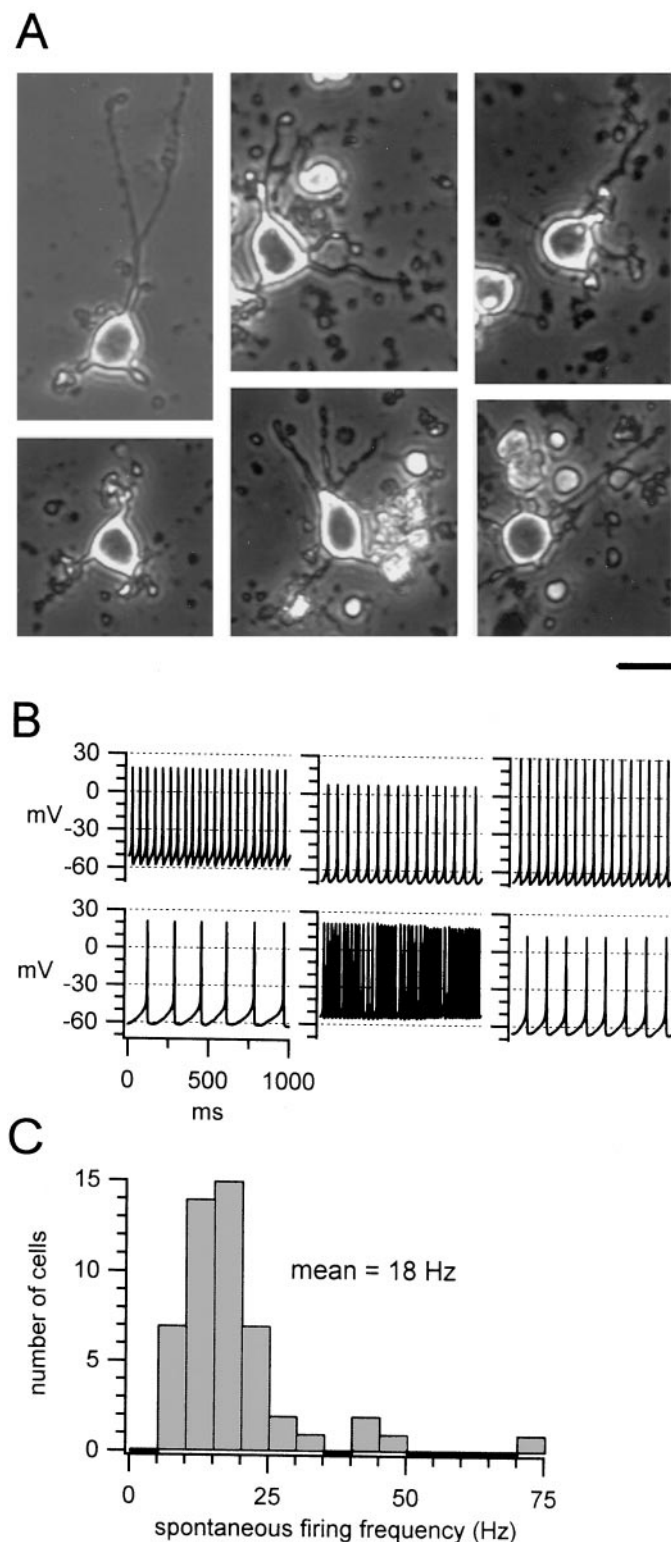


Figure 1. Spontaneous firing of neurons isolated from the cerebellar nuclei. *A*, Representative isolated cerebellar nuclear neurons. Scale bar, 20 μm . *B*, Spontaneous action potentials recorded from each of the six cells in *A*, all plotted on the same scale. Records are from cells in the corresponding positions in *A*. *C*, Histogram showing the distribution of firing frequencies in all of the cells that were tested ($n = 50$).

in part to a lower channel density in the isolated cells, possibly from the loss of distal dendrites or axons during the dissociation procedure or from the age of the animals that were used. Consistent with smaller total currents in isolated cells, the rate of rise of action potentials of isolated cerebellar nuclear neurons was approximately

fourfold lower (see below) than that measured in slices from adult guinea pigs (~ 400 V/sec; Jahnsen, 1986a). The lower temperature of the recordings also may have reduced the maximal measured spike rate in isolated cells.

Application of hyperpolarizing current steps such as those of Figure 2*B* allowed for the estimation of the input resistances of the neurons. The mean input resistance measured between -70 and -120 mV was 632 ± 40 M Ω ($n = 36$). This value is similar to that measured in rat cerebellar slices with patch electrodes (160–1900 M Ω ; Czubyko et al., 1998), but it is ~ 10 -fold greater than that measured in slices with intracellular microelectrodes (Jahnsen, 1986a; Aizenman and Linden, 1999). The firing frequency did not correlate with input resistance, as shown in Figure 2*C* (open circles).

Some neurons were not spontaneously active but rested at relatively depolarized potentials of -34 ± 2 mV ($n = 7$). Our initial concern was that these “silent” neurons might have become damaged and “leaky” during the isolation procedure. As shown in Figure 2*C*, however, silent neurons had input resistances indistinguishable from those of spiking neurons. In silent neurons, the input resistance measured between -70 and -120 mV was 699 ± 78 M Ω ($n = 7$; $p = 0.5$, unpaired t test with spontaneous cells), making it seem unlikely that the cells were unhealthy in this respect. Moreover, silent cells could be induced to fire regular trains of action potentials by the injection of steady hyperpolarizing currents of -10 to -60 pA, as illustrated in Figure 2*D*. These cells showed the same patterns of response to superimposed depolarizing current steps as spiking cells. In general, silent cells resembled spiking cells that already had reached a state of depolarization block. Occasionally, during the course of a recording an initially spontaneously active cell could depolarize slightly and become silent or hyperpolarize slightly and measurably reduce its firing rate.

Under the recording conditions of Figures 1 and 2, both E_K and E_{Cl} were near -90 mV. Therefore, the relatively shallow interspike troughs of spiking cells and depolarized resting potentials of silent cells, as well as the maintenance of firing during small hyperpolarizing current injections, suggest that inward currents are significantly active between spikes or at rest. To identify the currents that are likely to be active during spontaneous firing, we recorded voltage-clamped intrinsic currents of cerebellar nuclear neurons.

TTX-sensitive sodium currents

TTX-sensitive, voltage-gated transient sodium currents underlie action potentials in nearly all central neurons that have been studied. Additionally, components of TTX-sensitive sodium current that are less susceptible to inactivation appear to drive spontaneous action potentials in several cell types (Pennartz et al., 1997; Feigenspan et al., 1998; Bevan and Wilson, 1999; Raman and Bean, 1999). Furthermore, current-clamp studies have led to the suggestion that cerebellar nuclear neurons have a TTX-sensitive persistent sodium conductance that facilitates repetitive firing (Jahnsen, 1986a; Llinás and Mühlethaler, 1988). Such a current also might lead some cells to rest near -35 mV. We therefore recorded TTX-sensitive currents in isolated cerebellar nuclear neurons, with an interest in two general questions. First, how do the inactivation and recovery kinetics of TTX-sensitive currents interact to maintain firing? Second, how much TTX-sensitive current is active in the interspike interval, and is it crucial to depolarize neurons above threshold?

The first set of experiments was performed with solutions that facilitate the measurement of sodium currents, namely, intracellular CsCl and reduced extracellular sodium (50 mM NaCl). A family of TTX-sensitive currents evoked by step depolarizations from -90 mV is illustrated in Figure 3*A*, along with the corresponding peak current–voltage relation in Figure 3*B*. Extrapolation of the linear portion of the current–voltage relation, generally at potentials equal to or greater than -5 mV, allowed the estimation of the reversal potential (Fig. 3*B*, solid line). Normalization of the peak current by the driving force allowed the conversion of these data to

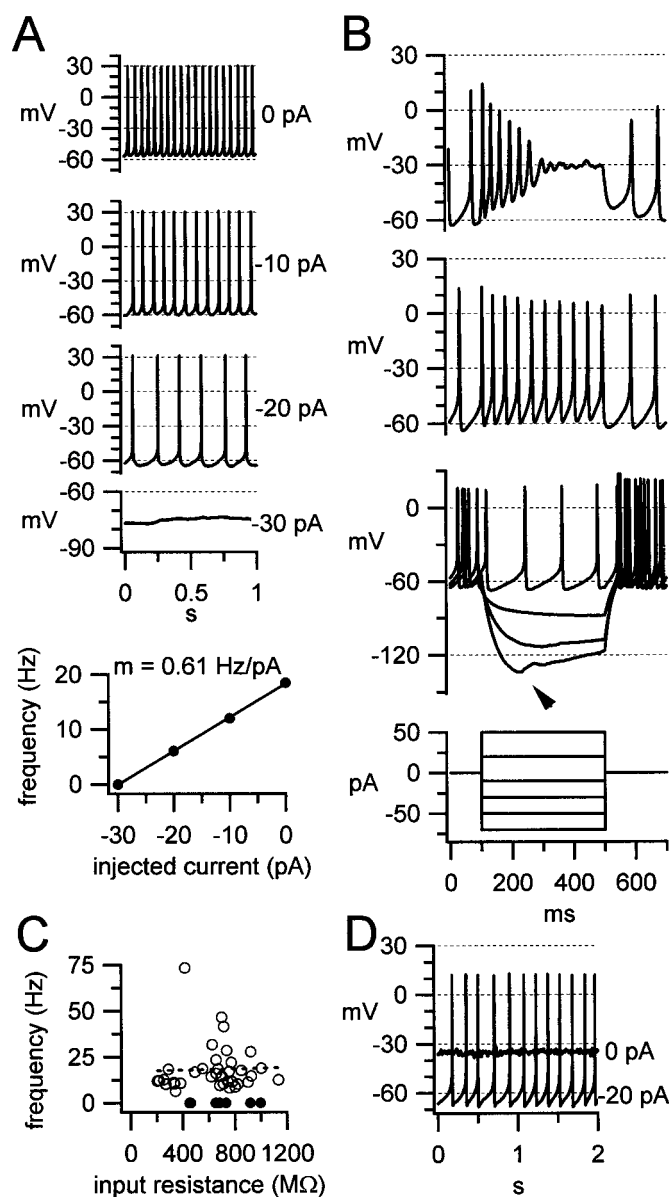


Figure 2. Firing patterns evoked by current injections. *A, Top*, Spontaneous firing and responses to steady injections of hyperpolarizing current, as labeled, of a single neuron. *A, Bottom*, Firing frequency versus injected current for the same neuron; $R^2 = 0.9997$. *B*, Responses of a different neuron to depolarizing and hyperpolarizing current steps. *First panel*, Depolarization block elicited by a 50 pA depolarizing step. *Second panel*, Increased firing rate with a 20 pA depolarizing step. *Third panel*, Input resistance (672 M Ω), as measured with hyperpolarizing current steps. For clarity, not all of the traces that were used to calculate input resistance are shown. The arrow indicates depolarizing sag. *Fourth panel*, Current steps. *C*, Firing frequency versus input resistance for seven "silent" neurons (filled symbols) and 36 spontaneously firing cells (open symbols). Firing frequency of spontaneous cells did not correlate with input resistance (line, $R^2 = 0.0008$). *D*, Resting potential of a silent neuron (-35 mV) and regular firing induced by a 20 pA injection of steady hyperpolarizing current.

conductances (Fig. 3C, open symbols). Boltzmann fits to the data from each cell gave a voltage of half-maximal activation of $-34.8 \pm 2.2 \text{ mV}$ and slope factor of $6.0 \pm 0.6 \text{ mV}$ ($n = 5$). Steady-state inactivation was assessed with 200 msec conditioning pulses, followed by test depolarizations to 0 mV. The resulting availability curve also is plotted in Figure 3C (closed symbols). Boltzmann fits estimated half-inactivation at $-68.6 \pm 1.5 \text{ mV}$, with a slope factor of $5.7 \pm 0.3 \text{ mV}$ ($n = 5$).

The availability of transient sodium currents before each action potential depends on at least two factors: the steady-state availability at interspike potentials and the time course of recovery from

inactivation that accumulates during each spike. Using standard step protocols, we measured recovery from inactivation at -65 mV . Cells were held at -90 mV to promote maximal availability of sodium channels. Then a 5 msec conditioning step to 0 mV was applied to inactivate the channels. After a variable interval at -65 mV , recovery was assessed with a test pulse to 0 mV (Fig. 3D,E). Currents recovered by $54 \pm 5\%$ ($n = 4$), consistent with the prediction from the steady-state availability curve, with a mean time constant of recovery of $11.4 \pm 1.9 \text{ msec}$.

Because the neurons have a minimum interspike potential near -60 mV and a mean interspike interval of $\sim 50 \text{ msec}$, these kinetic properties suggest that spontaneously firing neurons may operate with considerably $<50\%$ availability of TTX-sensitive channels. To obtain a more direct measure of the TTX-sensitive currents active during firing, we elicited currents with a spike-train command waveform consisting of 10 prerecorded action potentials. The waveform was chosen to approximate the mean firing rate (18 Hz) and trough potentials (-65 mV) of the population of neurons that we studied. Unlike the experiments of Figure 3, these recordings were made with physiological intracellular and extracellular solutions (KCH₃O₃S and control Tyrode's \pm TTX). Under these conditions both inward and outward currents are large (often $>10 \text{ nA}$) and fast (rising in $<1 \text{ msec}$), making it difficult to obtain adequate clamp in many cells. Nevertheless, in four neurons we were able to achieve a high-quality voltage clamp, assessed by the accurate subtraction of outward current in the TTX-subtracted records (Raman and Bean, 1999).

Cells were held at -68 mV in the 2 sec interval between spike-train commands. Holding at this voltage predicts a 50% availability of sodium channels before the application of the spike-train command. Therefore, the peak sodium current elicited by the first spike command provides an estimate of the current arising from 50% of the channels. Figure 4A illustrates that the peak TTX-sensitive current diminished with the first four or five successive spike commands, suggesting a cumulative inactivation. Because the initial availability was $\sim 50\%$, the availability just preceding the fifth spike is probably $<50\%$. After the fifth spike command, however, each spike command elicited a relatively constant amount of transient current. This result suggests that, after the fifth depolarization, inactivation during the spike command was equivalent to recovery between spike commands, such that a constant availability was achieved before each successive spike command.

A complicating factor in this analysis, however, is that the spike-train command that we used is unlikely to correspond exactly to the natural firing frequency of each cell. Consequently, if the spontaneous action potentials differ from the spike command depolarizations in rate or waveform, we might overestimate (or underestimate) the level of inactivation of TTX-sensitive currents before each spike during (unclamped) firing. To estimate this extent of inactivation in another way, we voltage-clamped neurons (using the bridge amplifier; see Materials and Methods) for 1–2 sec at -68 mV to promote a 50% availability of TTX-sensitive currents. Then we released the voltage clamp, recorded the onset of spontaneous firing, and calculated the time derivative of the voltage changes (dV/dt), which should be proportional to the underlying ionic current (Fig. 4B). The maximal rate of rise of the action potentials before reaching a steady level of $110 \pm 16 \text{ V/sec}$ ($n = 8$). Multiplying the measured dV/dt of 110 V/sec by the average cell capacitance of $\sim 20 \text{ pF}$ predicts an underlying ionic current of -2.2 nA . This value is somewhat greater than, but within the range of, the amplitude of transient TTX-sensitive currents ($-1.3 \pm 0.4 \text{ nA}$; $n = 4$) that we measured late in the spike-train commands. Together, the voltage- and current-clamp results support the idea that the sodium channel availability preceding each spike is $<25\%$.

This apparently low availability raises the possibility that steady hyperpolarization might recruit a significant number of sodium channels. To examine this idea, we evoked TTX-sensitive currents with the spike-train command, with and without a 10 mV hyper-

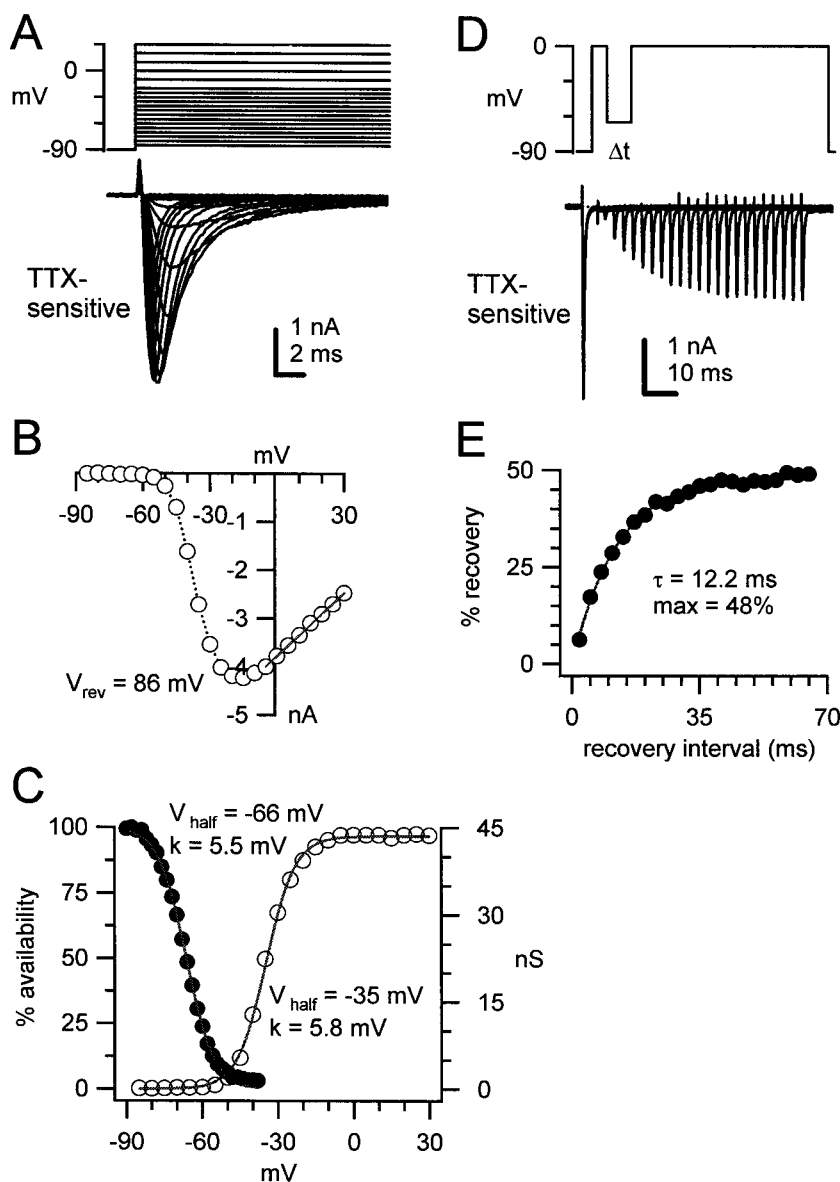


Figure 3. TTX-sensitive sodium currents elicited by step depolarizations. *A*, TTX-sensitive sodium currents evoked by step depolarizations from -90 mV in 2 mV increments. For clarity, only alternate traces are shown positive to -20 mV. *B*, Peak current versus voltage relation of traces in *A*. Solid line is a straight line fit to the linear portion of the curve from which the reversal potential, V_{rev} , was extrapolated. *C*, Conductance–voltage relation (open symbols) and steady-state availability curve (closed symbols) for the neuron for which the responses are illustrated in *A*. Activation data were fit as $G = G_{max}/(1 + \exp[-(V - V_{half})/k])$, where G_{max} is the maximal conductance, V_{half} is the half-maximal activation voltage, and k is the slope factor. Inactivation (availability) data were fit as the % availability = $100/(1 + \exp[(V - V_{half})/k])$, where the percentage of availability is the current evoked at 0 mV after a 200 msec conditioning step that is normalized by the maximal current evoked at 0 mV after conditioning at -90 mV, V_{half} is the half-maximal inactivation voltage, and k is the slope factor. Parameters of the fits are indicated on the plot. *D*, Recovery from inactivation of TTX-sensitive sodium currents. The variable recovery interval at -65 mV, Δt , ranged from 2 to 68 msec, in 3 msec increments. In this and all other figures of currents, the horizontal dashed line indicates 0 pA. *E*, Time course and extent of recovery of transient current shown in *D*. The peak current evoked by the test step to 0 mV was normalized to the peak current evoked by the conditioning step to 0 mV and was plotted against the recovery interval. Data were fit with a single exponential that estimated a maximum of 48% recovery, with a time constant of recovery, τ , of 12.2 msec.

polarizing DC shift. The peak current evoked by the ninth spike command occurred at 5.5 mV with the control waveform and at -1.5 mV with the DC-shifted waveform, 150 and 200 μ sec after the maximal dV/dt of the respective waveforms. Dividing the peak current by the driving force (from the empirically determined reversal) showed that the control waveform elicited a peak transient conductance of 3.6 nS, compared with 22 nS for the DC-shifted waveform (Fig. 4C). These values correspond to ~ 3.5 and 20% , respectively, of the total TTX-sensitive conductance of this neuron, estimated with step depolarizations from -90 to 0 mV. In a second cell the control and the DC-shifted waveforms evoked 2 and 12.5% , respectively, of the total TTX-sensitive conductance of the cell. Thus, a 10 mV hyperpolarization produced an approximately six-fold increase in conductance. This increase is likely to result in part from the greater maximal availability at more negative potentials and in part from the increase of recovery rate with hyperpolarization (Hodgkin and Huxley, 1952; Kuo and Bean, 1994).

The same set of experiments allowed us to study steady-state or long-lasting sodium currents. This component of TTX-sensitive current was measured after the decay of transient currents (90 – 200 msec after the onset of each step depolarization). In 50 mM NaCl the steady current was -22 ± 5 pA at -60 mV, and -50 ± 16 pA at -30 mV ($n = 7$; Fig. 5A). The channels responsible for this current may include (1) true persistently active channels (Llinás

and Sugimori, 1980; French et al., 1990; Kay et al., 1998; Magistretti et al., 1999a,b), (2) inactivating channels in noninactivating gating modes (Patlak and Ortiz, 1986; Alzheimer et al., 1993; Crill, 1996), and (3) inactivating channels with some equilibrium occupancy of an open state (Patlak and Ortiz, 1986; Raman et al., 1997). The total TTX-sensitive current that is active in the interspike interval, therefore, will depend on the amount of inactivation that may occur during a spike. Specifically, if most of the long-lasting current measured with voltage steps arises from a channel capable of fast inactivation, the TTX-sensitive current flowing between spikes may be less than that predicted by depolarizations to the interspike potential. Conversely, if most of the current arises from a persistently active channel, the interspike TTX-sensitive current should be approximately equivalent to that measured with step depolarizations. We therefore examined the current flowing on repolarization to -60 or -65 mV, after 5 msec steps to 0 mV. On repolarization, two of five cells showed a small phase of resurgent sodium current (Raman and Bean, 1997), which decayed within 10 msec (Fig. 5B). The steady TTX-sensitive current in 50 mM Na^+ , after the decay of any resurgent current, was -5.1 ± 1.3 pA ($n = 5$), smaller than the steady-state currents elicited by step depolarizations to the same potential. These results suggest that the majority of the channels that produced steady TTX-sensitive cur-

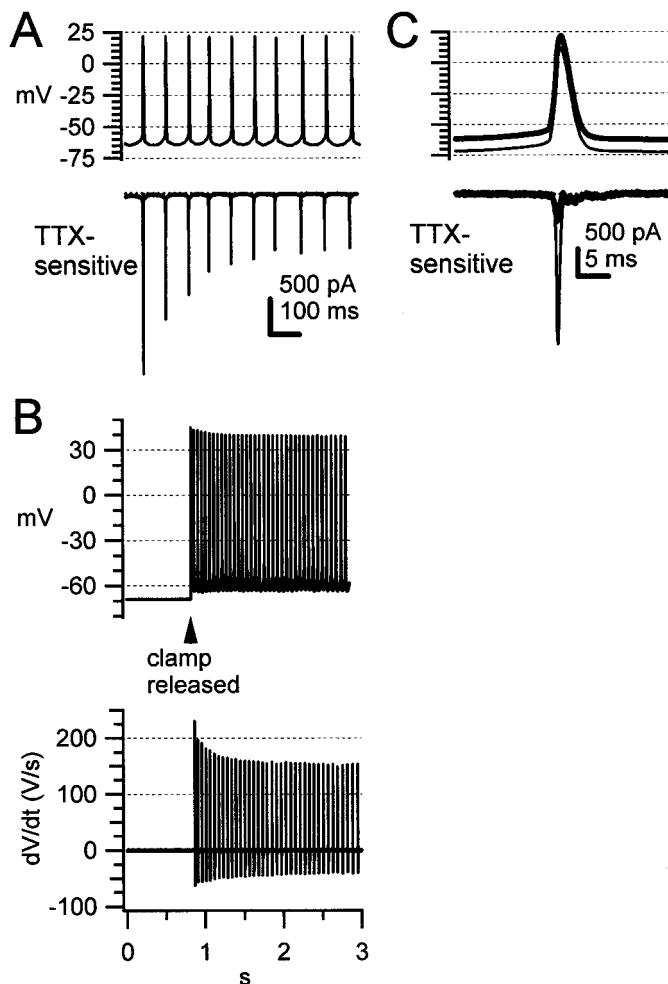


Figure 4. TTX-sensitive sodium currents evoked with spike-train command waveforms. *A, Top*, Voltage-clamp command waveform, consisting of a prerecorded train of spontaneous action potentials with average frequency, peak potential, and trough potential. *A, Bottom*, Mean TTX-sensitive current elicited by five spike-train commands. The intersweep holding potential was -68 mV for 2 sec. *B, Top*, Resumption of spontaneous firing after release from voltage clamp at -68 mV. *B, Bottom*, Differentiation of the current-clamp record, showing the decrease in peak dV/dt of each spike over the first 10–15 action potentials. *C, Top*, The ninth action potential waveform of the spike-train command (*A*), with (*thin trace*) and without (*bold trace*) a 10 mV DC hyperpolarization. *C, Bottom*, TTX-sensitive current evoked by the control (*thin trace*) and DC-shifted (*bold trace*) voltage command. This is a different cell from *A*.

rents in response to long depolarizing steps to -60 mV inactivated within milliseconds at more positive potentials.

To estimate how much TTX-sensitive sodium current flows during interspike intervals in normal concentrations of sodium ions, we examined the TTX-sensitive current that was recorded in physiological saline (Fig. 5C). This current, averaged over a 15 msec interspike interval in which the membrane potential was close to -60 mV, was -9 ± 6 pA ($n = 4$).

The contribution of this apparently small current to depolarizing the neuron cannot be assessed in voltage clamp. Therefore, we measured the resting potentials of current-clamped neurons for which the spontaneous firing was blocked by TTX (Fig. 5D). Surprisingly, in TTX, these neurons rested at -42 ± 2 mV ($n = 15$). This value is significantly more positive than either the interspike trough in the absence of TTX (-61 ± 1 mV; $p = 0.0000002$) or threshold (-49 ± 1 mV; $p = 0.003$), estimated as the onset of the regenerative phase of the action potential, suggesting that TTX-insensitive currents alone can depolarize neurons to potentials that normally would be suprathreshold.

Potassium and calcium currents

Calcium currents are likely candidates for depolarizing neurons in TTX to potentials near -40 mV. Therefore, to measure the effects of calcium influx on firing, we recorded from current-clamped neurons in control Tyrode's and in Co Tyrode's, in which calcium flux was blocked by complete substitution by cobalt ions. Ten of 11 spontaneously firing neurons were silenced in Co Tyrode's, resting at -52 ± 4 mV; the 11th neuron continued to fire sporadically. Although the resting potentials were somewhat more negative in Co Tyrode's than in TTX ($p = 0.04$, unpaired t test), silenced neurons rested above threshold (Fig. 6A), suggesting that the cessation of firing did not result from a lack of depolarizing drive. When cells were tonically hyperpolarized with small current injections, spontaneous firing did not occur, but depolarizing current steps could elicit action potentials. In Co Tyrode's, the neurons entered depolarization block even more readily than in control solutions (Fig. 6B). To quantify this effect, we measured the peak and trough of the first action potential elicited by a 40 or 50 pA depolarizing step in each solution. In Co Tyrode's, the peak amplitude of the first action potential did not change significantly relative to control, depolarizing by 0.2 ± 2 mV ($n = 10$; $p = 0.92$). In contrast, the subsequent trough depolarized by 6 ± 1 mV in Co Tyrode's ($n = 10$; $p = 0.0005$). It is possible that the shallower interspike troughs in cobalt reduce the recovery of TTX-sensitive sodium channels, which may lead to the termination of firing. The apparent loss of hyperpolarizing drive suggests that calcium-dependent currents, possibly K(Ca) currents, contribute strongly to the repolarization of action potentials.

Evidence from slice studies suggests that K(Ca) channels contribute to the firing patterns of cerebellar nuclear cells (Jahnsen, 1986b; Aizenman and Linden, 1999). Specifically, the blockade of SK channels by bicuculline methiodide (BMI; Khawaled et al., 1999) can induce burst firing of cerebellar nuclear neurons in slices (Aizenman and Linden, 1999). In contrast, although application of $100 \mu\text{M}$ BMI to isolated cells modified the waveform of the interspike interval, the firing rate changed by only 1.4 ± 1.7 Hz ($n = 7$; $p = 0.84$) and never induced bursting (Fig. 6C,D). Taken together, the experiments of Figure 6 suggest that K(Ca) currents other than BMI-sensitive SK channels may participate in spike repolarization.

To study the density and kinetics of currents that might participate in spike repolarization of the isolated cells, we measured calcium and potassium currents under voltage clamp. Recordings were made with physiological internal and external solutions, but with 900 nM TTX included extracellularly. Currents were evoked by step depolarizations from -68 mV as well as by the spike-train command waveform. As shown in Figure 7A (*top traces*), the steps elicited large, primarily outward currents that occasionally were preceded by a small phase of inward current. The total current had a fairly high threshold for activation, with outward currents becoming detectable (>10 pA) between -45 and -35 mV ($n = 7$; Fig. 7B). The spike waveforms of the spike-train command also elicited primarily outward currents (Fig. 7C). Between spike commands, however, a TTX-insensitive inward current of -39 ± 14 pA ($n = 7$) was measurable during the ~ 15 msec window when the membrane potential was near -65 mV (Fig. 7D, *top traces*).

We performed a simple pharmacological segregation of the total currents, again excluding TTX-sensitive sodium current, by repeating recordings in the following solutions: Co Tyrode's, control Tyrode's with 1 mM TEA (TEA Tyrode's), and Co Tyrode's and 1 mM TEA (Co + TEA Tyrode's). All solutions contained TTX. Currents sensitive to cobalt, TEA, or both were obtained by subtraction. Raw currents obtained in Co Tyrode's as well as the cobalt-sensitive current are shown in Figure 7, A and D. The cobalt-resistant step-evoked currents had a slower activation time and higher activation threshold than the cobalt-sensitive currents, which include calcium and calcium-activated currents. Additionally, the inward current between spike commands was reduced by -17 ± 10 pA in Co Tyrode's ($n = 4$; Fig. 7D).

The cobalt-sensitive and -resistant currents each had a TEA-sensitive component (Fig. 8A,B). The step-evoked and spike-train-

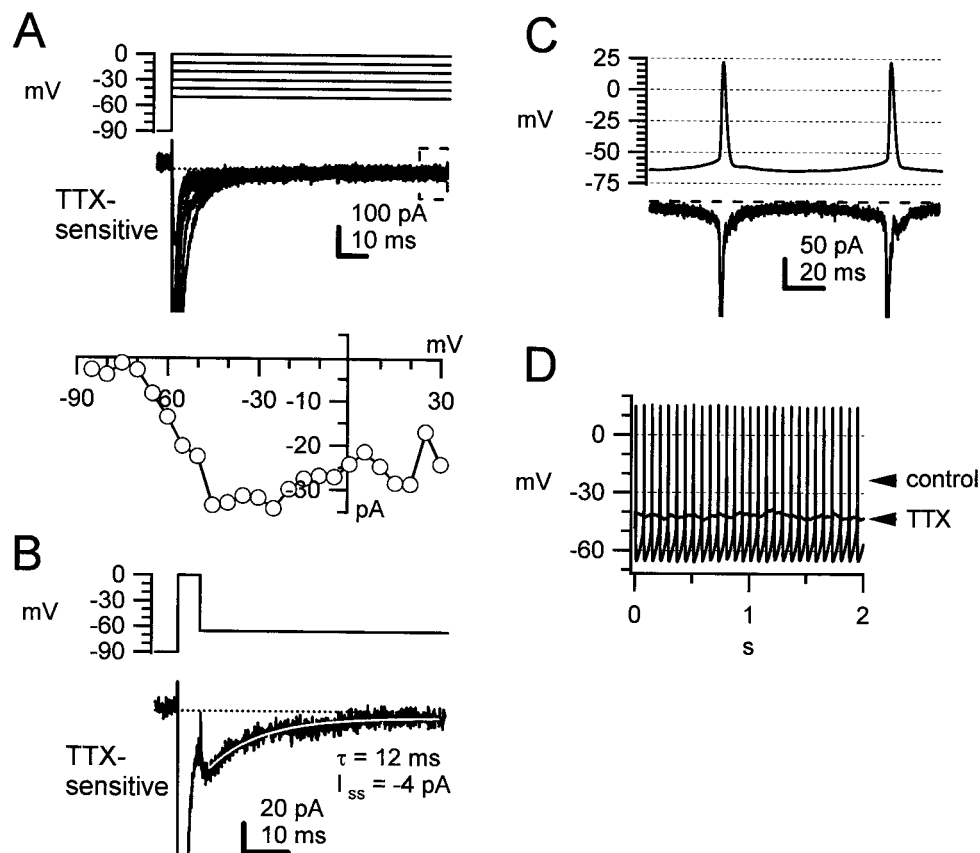


Figure 5. Long-lasting TTX-sensitive sodium currents. *A, Top*, TTX-sensitive sodium currents evoked by step depolarizations from -90 mV in 10 mV increments. *A, Bottom*, Current–voltage relation of the mean steady-state current measured between 90 and 100 msec (within the dashed box of the top panel). This is the same record as Figure 3*A*. *B*, Mean of the last three traces in Figure 3*D*, with recovery intervals of 62 , 65 , and 68 msec, expanded to illustrate the TTX-sensitive current on repolarization to -65 mV. The small resurgent sodium current decayed with an exponential time constant of 12 msec to -4 pA. *C*, Expansion of eighth and ninth spike command and evoked currents of Figure 4*A*, illustrating the interspike TTX-sensitive current. *D*, Current-clamp records of spontaneous firing in control Tyrode's and subsequent silencing on exposure to TTX, as labeled, in one neuron. In TTX the cell rested at -42 mV.

evoked currents are plotted on the same vertical scale to allow a comparison of the current amplitudes elicited by each protocol under each ionic condition. The top traces show the cobalt-insensitive, TEA-sensitive current. For brevity, we refer to this current as $K(V)_{TEA}$. Qualitatively, this current was a high-threshold delayed rectifier, which showed little or no inactivation during 100 msec step depolarizations. The $K(V)_{TEA}$ current had a half-maximal voltage of activation of $+8.6 \pm 3.7$ mV and slope factor of 10.6 ± 2.3 mV ($n = 4$; Fig. 8*C*). The 10 – 90% rise time of the current was 24 ± 4 msec at $+12$ mV ($n = 4$). Despite the relatively slow activation kinetics, $K(V)_{TEA}$ accounted for $51 \pm 3\%$ of the current evoked by the spike-train command.

The middle panels in Figure 8, *A* and *B*, illustrate the TEA-sensitive, calcium-dependent current, which we refer to as $K(Ca)_{TEA}$ and which was obtained by subtracting the $K(V)_{TEA}$ currents from the total TEA-sensitive current. This current had a half-maximal activation voltage of -14.3 ± 3.8 mV and a slope factor of 7.9 ± 0.7 mV ($n = 4$; Fig. 8*C*). At 12 mV, the current had an inactivating component with an exponential decay time constant of 12.3 ± 3.5 msec. The extent of inactivation varied greatly, from 38 to 91% , suggesting that there may be multiple components of $K(Ca)_{TEA}$.

Together, the TEA-sensitive currents accounted for $57 \pm 5\%$ of the maximal outward current elicited by a step from -68 mV to $+20$ mV ($n = 7$). In five of seven cells, however, TEA blocked all of the outward current elicited by the spike-train command. In the other two cells, TEA-sensitive currents accounted for 85 and 87% of the outward spike command-evoked current. On repolarization by the spike command, the total TEA-sensitive currents decayed with an exponential time constant of 2.0 ± 0.8 msec ($n = 7$).

Subtractions of the records obtained in Co + TEA Tyrode's from those in TEA Tyrode's allowed the isolation of calcium current plus any 1 mM TEA-insensitive $K(Ca)$, visible as an inward current followed by an outward current. Six of seven cells showed such a TEA-insensitive $K(Ca)$ of 348 ± 68 pA net current at $+20$ mV (Fig. 8*A*, bottom traces). The seventh cell had an unusually

large TEA-insensitive $K(Ca)$ of 2 nA net current at $+20$ mV. As mentioned above, this outward current was elicited infrequently by the spike-train command (in two of seven cells, accounting for $<15\%$ of the outward current). More often, only the inward phase of calcium current was apparent (Fig. 8*B*, lowest panel).

I_h and other cation currents

Although TTX-sensitive sodium flux and calcium flux are crucial for firing, our data suggested that neither class of currents dominates depolarization of the neurons to suprathreshold voltages. Because an inward current of approximately -25 pA at -60 mV persisted in solutions containing both TTX and cobalt and because currents of this amplitude were sufficient to influence action potential firing in current-clamped neurons, we examined this residual current in more detail. We considered three possibilities. First, the current might be an I_h that was partly activated at approximately -65 mV, in which case we expect it to be blocked by external cesium and to show increasing activation with hyperpolarization. Second, the current might be a nonspecific leak current between the patch electrode and the cell, in which case we expect it to be insensitive to ion substitution and to reverse near 0 mV. Third, the current might result from another type of cation channel that has some permeability to sodium, in which case we expect it to be sensitive to replacement of sodium ions by a less permeant ion.

We began by studying I_h . In current-clamped neurons in physiological solutions, hyperpolarizing current steps to potentials more negative than -100 mV often evoked the depolarizing sag usually associated with I_h ($n = 29$ of 45 cells; see Fig. 2*B*, bottom traces, arrowhead). Other cells showed no I_h , even at these very negative potentials ($n = 16$). These observations suggest a low density of somatic I_h as well as a relatively negative voltage dependence of I_h activation. Consistent with this idea, recordings from cerebellar nuclear neurons in slices show a similarly negative hyperpolarization-evoked sag and occasionally no sag at all (Jahnsen, 1986a; Aizenman and Linden, 1999).

To investigate the properties of I_h directly, we recorded the

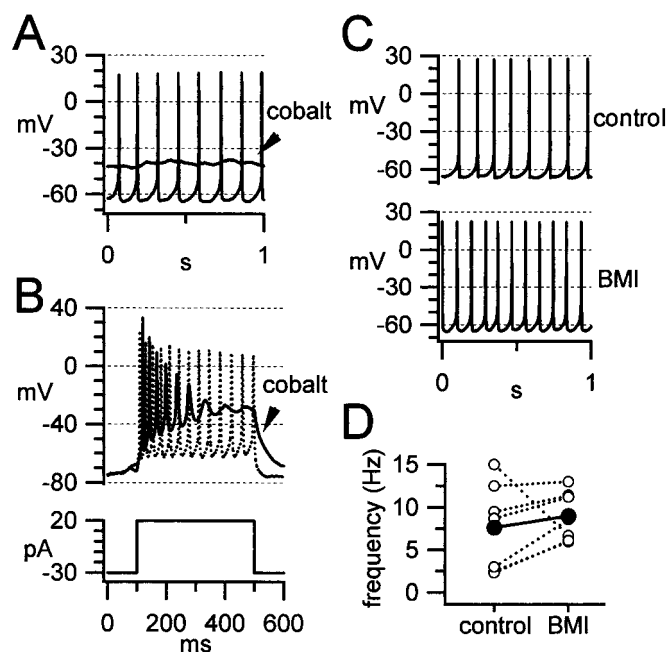


Figure 6. Firing patterns of neurons during blockade of calcium currents and calcium-activated currents. *A*, Spontaneous firing in control Tyrode's and subsequent silencing on exposure to Co Tyrode's. In Co Tyrode's the neuron rested at -37 mV. *B*, Responses in control Tyrode's (dotted line) and Co Tyrode's (solid line) to depolarizing current steps superimposed on a steady hyperpolarizing current. The peak amplitude of the first action potential depolarized by 9 mV in Co Tyrode's, and the trough depolarized by 7 mV. *C*, Spontaneous firing of a single neuron in control Tyrode's and in Tyrode's with $100 \mu\text{M}$ bicuculline methiodide (BMI). *D*, Firing frequencies of seven cells in control solutions and on exposure to $100 \mu\text{M}$ BMI (open symbols). Closed symbols show the mean data.

current under voltage clamp. In physiological intracellular solutions and extracellular control Tyrode's with TTX, neurons were clamped at -48 mV, and 500 msec step hyperpolarizations were applied. A small inward current activated slowly at potentials negative to -90 mV and was blocked by 2 mM CsCl. Cesium-sensitive current is shown in Figure 9*A* (top traces). The amplitude of this current after 400 – 500 msec at -120 mV was -29 ± 8 pA ($n = 6$; Fig. 9*B*).

At least three factors may lead us to underestimate the density of I_h in cerebellar nuclear neurons. First, in some neurons, I_h is expressed preferentially in distal dendrites (Magee, 1998; Williams and Stuart, 2000), which are reduced in the dissociated cell preparation. Second, I_h channels have been shown to be sensitive to enzymatic cleavage by trypsin (Budde et al., 1994), although the current has been recorded successfully in some papain-dissociated cells (Tabata and Ishida, 1996). Third, the voltage dependence of I_h can be modulated by intracellular cAMP (Lüthi and McCormick, 1999), which may be submaximal under our recording conditions.

As a control for the effects of papain as well as for our recording conditions, we isolated bushy cells from the ventral cochlear nucleus of age-matched mice. The dissociation procedure was identical to that for cerebellar nuclear neurons. These neurons were selected as a control because they are known to have I_h , despite their limited dendritic arbor (Cant and Morest, 1979; Oertel, 1983). In all of the cells, an inward cesium-sensitive current was evoked on hyperpolarization. The cesium-sensitive current amplitude after 400 – 500 msec at -120 mV was -146 ± 36 pA ($n = 5$; Fig. 9*A,B*), approximately five times the amplitude in cerebellar nuclear neurons. Although these data do not rule out a reduced current density as a consequence of the dissociation procedure in either cell type, they support the idea that cerebellar nuclear neurons have a relatively low density of somatic I_h . Additionally, the slow activation kinetics and negative voltage dependence in these cells suggest that I_h is unlikely to dominate the inward

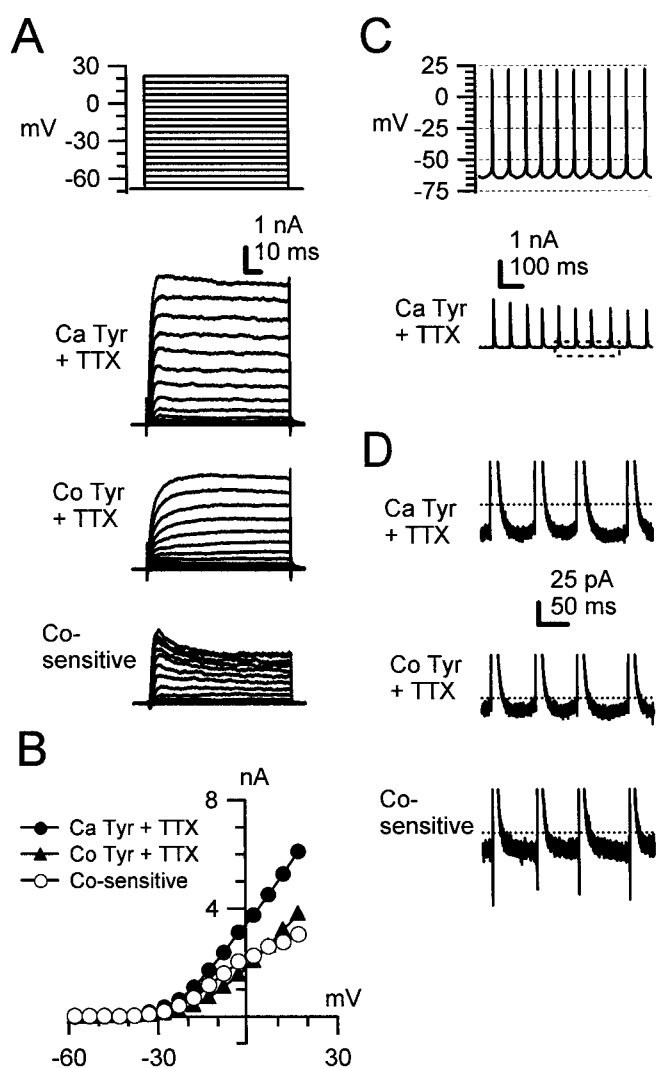


Figure 7. Total TTX-insensitive currents evoked by step and spike-train voltage-clamp commands in physiological solutions. *A*, Top, Middle, Raw currents evoked by step depolarizations in control Tyrode's with TTX (Ca Tyr + TTX) and Co Tyrode's with TTX (Co Tyr + TTX). *A*, Bottom, Cobalt-sensitive currents, obtained by subtraction of the currents in the top and middle panels. *B*, Current-voltage relation of peak currents in *A*. *C*, Raw current elicited by the spike-train command in control Tyrode's with TTX. Intersweep holding potential was -68 mV for 2 sec; mean of five sweeps. *D*, Top, Expansion of current within dashed lines in *C* to illustrate TTX-insensitive inward current at interspike potentials. *D*, Middle, Currents evoked in Co Tyrode's by the spike-train command. The illustrated portion of the record corresponds to that shown in the top panel. *D*, Bottom, Cobalt-sensitive currents, obtained by subtraction of currents in the top and middle panels.

current active at interspike potentials (mean current -3 ± 0.9 pA at -58 mV; $n = 5$).

To test the ion selectivity of the small tonic current, we applied step hyperpolarizations from -58 mV to cells that were exposed first to control Tyrode's + TTX (155 mM Na^+) and then to NMDG-Tyrode's + TTX (6 mM Na^+ ; see Materials and Methods). The resulting currents were small and linear. Reducing external sodium ions significantly reduced the steady currents at all potentials (Fig. 10*A*). The extrapolated reversal potential was shifted negatively by 20 ± 2.3 mV, from -34 ± 2.5 mV in normal sodium to -54 ± 1.4 mV in low sodium ($n = 8$; $p = 0.00005$; Fig. 10*B,C*). The reversal potential in normal sodium is close to the resting potentials of current-clamped neurons exposed to TTX. Additionally, the slope decreased to $67 \pm 6\%$ of control. Repeating the experiments with 2 mM Cs^+ added to the control Tyrode's and NMDG-Tyrode's solutions produced similar results. With cesium present the reversal potential was shifted negatively by 24 ± 6 mV,

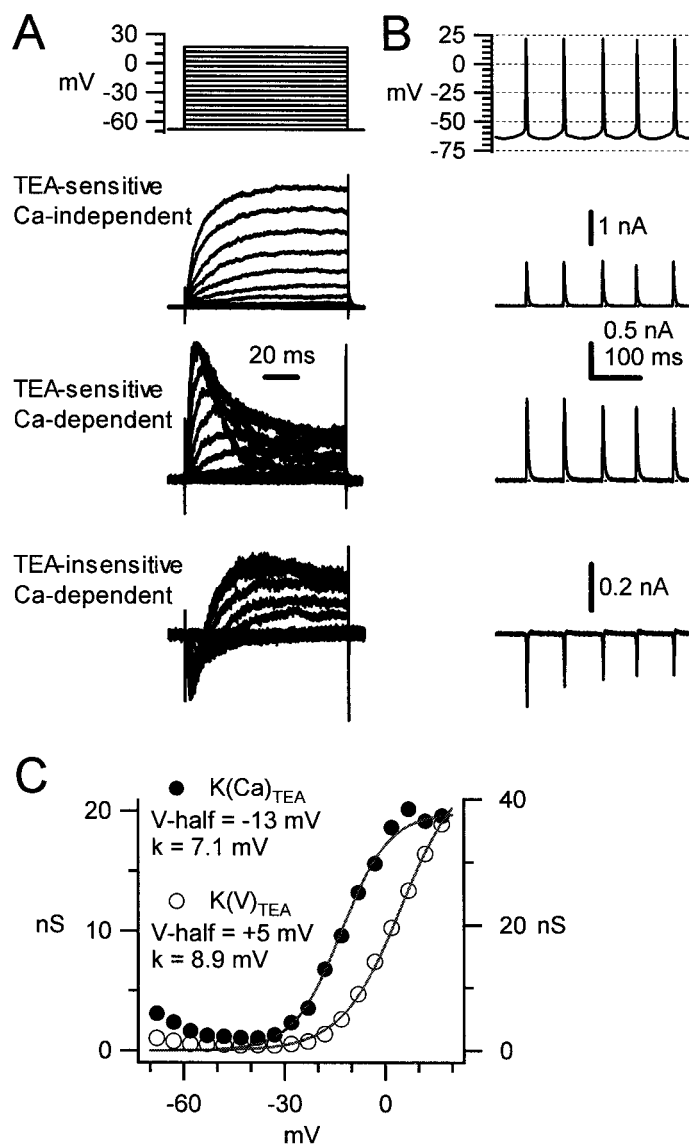


Figure 8. Potassium currents pharmacologically isolated with cobalt substitution and 1 mM TEA. *A, B*, Currents evoked by step and spike-train voltage-clamp commands (*top panels*). Time scale bars in *A* and *B* apply to all panels in *A* and *B*, respectively. Vertical scale bars in *B* apply to the corresponding panels in *A*. Currents evoked by spike-train commands are the mean of five traces. Intersweep holding potential was -68 mV for 2 sec. This is a different cell from Figure 6. *Top trace*, Calcium-independent current, sensitive to 1 mM TEA, also referred to as $K(V)_{TEA}$. *Middle traces*, Calcium-dependent current, sensitive to 1 mM TEA, also referred to as $K(Ca)_{TEA}$. *Bottom trace*, Calcium-dependent current, resistant to 1 mM TEA (including calcium and calcium-activated potassium currents). Note that little outward current is measured between spike commands in response to the spike-train protocol. *C*, Conductance-voltage relation for peak $K(Ca)_{TEA}$ currents (filled symbols) and peak $K(V)_{TEA}$ currents (open symbols). Data were fit with Boltzmann equations as in Figure 3B, and the estimated parameters are indicated in the plot.

from -5.2 ± 4.6 to -30 ± 2.7 mV ($n = 6$; $p = 0.01$; Fig. 10*B*), and the slope became $60 \pm 10\%$ of control. When currents were evoked by the spike-train command in NMDG-Tyrod's (containing TTX), the interspike current was reduced to near 0 pA in NMDG-Tyrod's (Fig. 10*D*). Thus the standing current near -60 mV and at interspike potentials appears to be ion-selective, with some permeability to Na^+ . This result suggests that it may be carried through an ion channel (or channels) rather than being a nonselective leak between electrode and cell. The reversal near -35 mV, as well as the -20 mV shift of reversal with ~ 25 -fold reduction in Na^+ , suggests that other ion(s) also may permeate the putative channel.

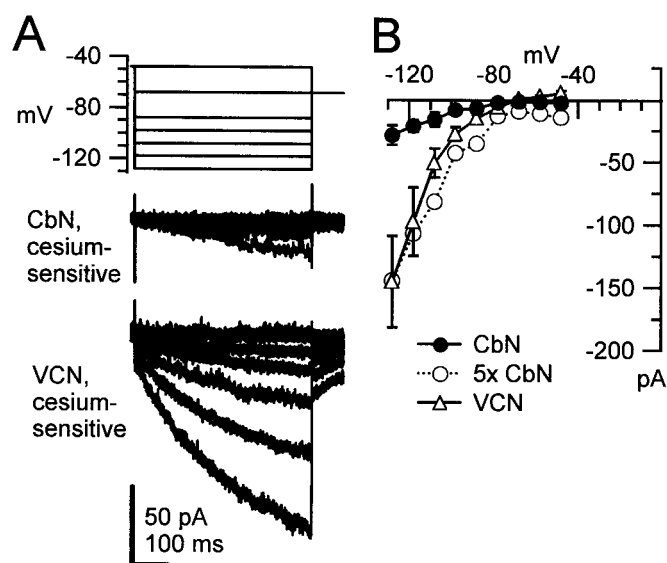


Figure 9. I_h in cerebellar nuclear neurons and in bushy cells of the ventral cochlear nucleus. *A*, Currents were elicited by 500 msec hyperpolarizing steps from -48 mV in -10 mV increments. I_h was isolated by subtraction of the records in Tyrod's with 2 mM CsCl from those in control Tyrod's. *A, Top traces*, Cesium-sensitive current recorded from a cerebellar nuclear neuron (CbN). *A, Bottom trace*, Cesium-sensitive current recorded in a bushy cell from the ventral cochlear nucleus (VCN). *B*, Mean current between 400 and 500 msec versus voltage for cerebellar nuclear neurons (filled circles; $n = 6$) and ventral cochlear nucleus neurons (open triangles; $n = 5$). Five times the mean current for cerebellar nuclear neurons is plotted for comparison ($5 \times$ CbN, open circles).

Cationic fluxes have been described in hippocampal interneurons (McQuiston and Madison, 1999a,b) and pyramidal neurons (Guérineau et al., 1995). In both of these cell types, cationic currents contribute to afterdepolarizations, vary with the concentration of external sodium ions, and can be enhanced by muscarine and/or ACPD. Measured with the step hyperpolarizations shown in Figure 10, however, the tonic current of cerebellar nuclear cells was unchanged by 3 min exposures to muscarine ($40 \mu M$; $n = 5$) or ACPD ($50 \mu M$; $n = 2$). It also was unaffected by 8-Br cAMP ($50 \mu M$; $n = 5$), 8-Br cGMP ($50 \mu M$; $n = 4$), or benzamil ($50 \mu M$; $n = 5$), a blocker of the Na/Ca exchanger (data not shown). Finally, although the extrapolated reversal potential of the current suggests a cation nonselectivity, we considered the possibility that the channel belonged to the bNaC family of amiloride-sensitive, voltage-independent sodium channels (Canessa et al., 1994; García-Añoveros et al., 1997; Benos and Stanton, 1999). Amiloride ($100 \mu M$) affected neither spontaneous firing nor resting potentials measured in TTX, however ($n = 5$; data not shown).

Ionic determinants of the resting potential and interspike depolarizations

We could not assess directly the contribution of the tonic TTX-insensitive flux to spontaneous activity by reducing the external Na^+ concentration, because replacement of Na^+ by NMDG also substantially reduced the amplitude of the TTX-sensitive sodium currents. Instead, we tested the contribution of various fluxes to the resting potentials measured in TTX. First, we recorded the spontaneous firing of neurons in control Tyrod's. Next, we silenced the cells with TTX and measured their resting potentials. Finally, we recorded any changes in resting potential as each cell was exposed to one or more of the following solutions, each containing TTX: (1) NMDG-Tyrod's, (2) Co Tyrod's, or (3) control Tyrod's with 2 mM CsCl. The only manipulation that significantly changed the resting potential was exposure to NMDG-Tyrod's (Fig. 11*A,B*), which hyperpolarized cells by 22 ± 2.8 mV, to -61 ± 3 mV ($n = 9$; $p = 0.00005$). In contrast, Co Tyrod's with TTX changed the membrane potential by -2.8 ± 1.7 mV, to -48 ± 3 mV ($n = 11$; $p = 0.12$). Control Tyrod's with cesium and TTX changed the

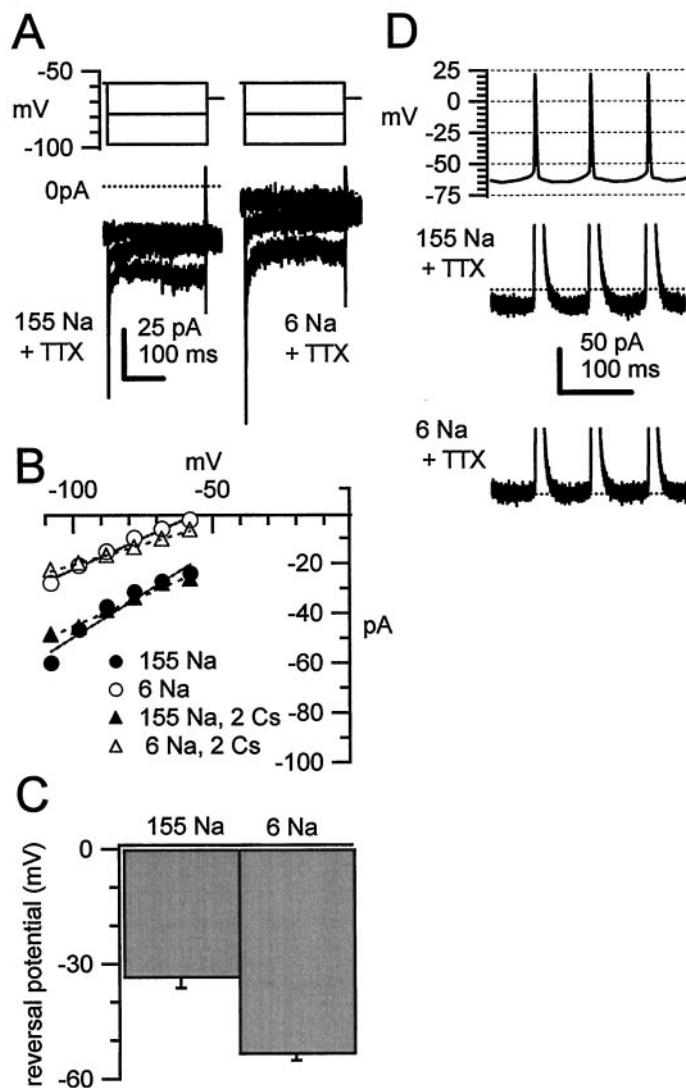


Figure 10. Reduction of TTX-insensitive steady inward current in low-sodium solutions. *A*, Raw currents evoked by 250 msec step hyperpolarizations. Holding potential is -58 mV. *A*, Left traces, Currents elicited in control Tyrode's with TTX. *A*, Right traces, Currents elicited in NMDG-Tyrode's with TTX. Scale bars apply to both panels. Shown are data from one cell. *B*, Current-voltage relations of mean currents in each panel of *A* (circles) as well as currents evoked by the same protocol in the same cell, recorded in solutions containing 2 mM CsCl (triangles). The lines indicate linear regression over the points, with (dashed lines) and without (solid lines) cesium present. *C*, Mean extrapolated reversal potential of currents analyzed as in *B*, in high (155 mM) and low (6 mM) sodium solutions ($n = 8$). *D*, Raw currents elicited by the spike-train command in control Tyrode's with TTX (top trace) and in NMDG-Tyrode's with TTX (bottom trace). Intersweep holding potential was -68 mV for 2 sec; mean of five sweeps.

membrane potential by -0.6 ± 2.5 mV, to -42.6 ± 6.7 mV ($n = 3$; $p = 0.8$). It therefore seems likely that the tonic TTX-insensitive sodium flux contributes strongly to depolarizing cerebellar nuclear neurons above threshold voltages.

DISCUSSION

Cerebellar nuclear neurons are the primary synaptic targets of Purkinje cells and the major output neurons of the cerebellum. Despite their important location, little is known about the biophysical mechanisms underlying their activity (Sastry et al., 1997). When isolated, these cells fire spontaneous action potentials similar to those in intact preparations (Thach, 1968; Jahnsen, 1986a; Llinás and Mühlethaler, 1988; Mouginot and Gähwiler, 1995; Aizenman and Linden, 1999) and therefore provide reasonable models for studying firing. Importantly, isolated cells allow for

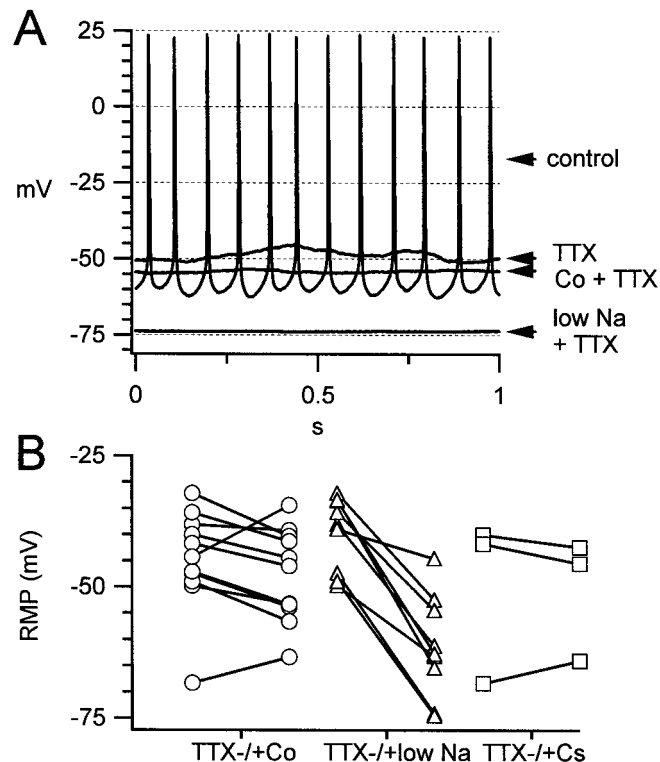


Figure 11. Dependence of the resting potential on extracellular sodium concentration. *A*, Spontaneous firing of a neuron in control Tyrode's (control) and resting potentials of the same cell on exposure to control Tyrode's with TTX (TTX), Co Tyrode's with TTX (Co + TTX), and NMDG-Tyrode's with TTX (low Na + TTX). *B*, Within-cell comparisons of resting membrane potentials (RMP) measured in Tyrode's with TTX and in one or more of the following solutions: Co plus TTX, low Na plus TTX, or control Tyrode's with TTX and 2 mM CsCl.

quantitative measurements of the pharmacology and kinetics of the ionic currents intrinsic to these neurons, which previously have not been studied under voltage clamp.

Currents that determine the resting potential

Potassium channels, including M-channels, inward rectifiers, and TASK channels, tend to bring resting potentials toward E_K (Marriott, 1997; Reimann and Ashcroft, 1999; Millar et al., 2000); in several cell types the Na/K pump also serves to hyperpolarize resting potentials (Jacob et al., 1987; Jones, 1989; Trotter and Døving, 1996). Many neurons rest positive to E_K , however, indicating that inward currents also must be active at rest (Forsythe and Redman, 1988; Jones, 1989). These can include I_h (Jones, 1989; Spruston and Johnston, 1992; Lamas, 1998; Doan and Kunze, 1999) and possibly other TTX-insensitive sodium fluxes (Forsythe and Redman, 1988). Additionally, the Na/Ca exchanger has been reported to depolarize resting potentials (Jacob et al., 1987).

In TTX, the cerebellar nuclear neurons rested ~ 50 mV positive to E_K , suggesting that potassium currents do not dominate sub-threshold potentials. I_h did not appear to contribute strongly to interspike depolarizations or rest in TTX, because little cesium-sensitive current flowed at potentials greater than or equal to -60 mV and depolarizing sags appeared only negative to -100 mV. These results are consistent with cerebellar nuclear expression of HCN2, but not HCN1, mRNA; the HCN2 channel has slower activation kinetics and activates at more negative voltages (Santoro et al., 2000). Resting currents also were unaffected by blocking the Na/Ca exchanger.

The major resting current (in TTX) appeared to be a tonic cationic flux, carried in part by sodium ions. The channels carrying this current may account for the resting permeability to sodium in many cells. The current appears electrophysiologically similar to background nonselective cation currents of cardiac cells (Hagiwara

et al., 1992; Manabe et al., 1995; Zhang et al., 2000). The existence of such a flux in cerebellar nuclear neurons is consistent with Jahnsen's (1986a) observation that the cells "always showed signs of having a steady inward current." By analogy to Purkinje neurons (Llinás and Sugimori, 1980), Jahnsen proposed that the depolarization resulted from persistent sodium currents. The tonic cation current, however, differs in at least three ways from "persistent sodium currents," as the term usually is used. First, persistent sodium currents are generally TTX-sensitive (French et al., 1990; Crill, 1996; Kay et al., 1998), which the tonic cation current is not. The TTX insensitivity suggests that the tonic cation current is a distinct molecular entity.

Second, the persistent sodium current activates just positive to -70 mV (Stafstrom et al., 1985; French et al., 1990; Cepeda et al., 1995), whereas the tonic cation current appears voltage-independent. Therefore, unlike persistent sodium current, the tonic cation current would tend to drive cerebellar nuclear neurons suprathreshold, even after significant hyperpolarization.

Third, the reversal potentials of the tonic cation current and persistent sodium current are distinct. Persistent sodium currents reverse near E_{Na} (Kay et al., 1998; Magistretti et al., 1999a), whereas the extrapolated reversal potential of the tonic cation current was near -30 mV. This reversal suggests that ions in addition to sodium, possibly potassium, permeate the channel. Assuming a single channel type permeant only to sodium and potassium, the reversal potential predicts a P_{Na}/P_K of 0.25. In that case, however, a 25-fold reduction of sodium should shift the reversal substantially more negative than was observed (predicted, -84 mV; observed, -53 mV). Possibly, voltage-gated calcium currents contribute to the total current measured negative to -40 mV, or calcium may permeate the putative channel, shifting the reversal positive, particularly in low-sodium solutions. Consistent with calcium permeability, cobalt substitution reduced the tonic inward current even below -90 mV, where little voltage-gated current is expected to be active (data not shown). Alternatively, cobalt simply may block the putative cation channel. Finally, some proportion of the total tonic inward current at -60 mV may result from calcium-activated nonselective (CAN) cation currents (Yellen, 1982; Swandulla and Lux, 1985; Hasuo et al., 1990; Wilson et al., 1996). CAN channels cannot account completely for the inward current, however, because resting potentials remained near -50 mV with cobalt substituted for calcium.

Recently, a calcium-dependent increase in the intrinsic excitability of cerebellar nuclear neurons has been demonstrated (Aizenman and Linden, 2000). Because the firing frequency of the cells varies linearly with current injections, changes in the amplitude of the tonic cation conductance might influence firing rates. The tonic cation current therefore may provide one substrate for modulation of the excitability of cerebellar nuclear neurons.

Sodium currents

The activation, inactivation, and recovery kinetics of TTX-sensitive transient sodium currents were similar to those of other central neurons (Sah et al., 1988; Kuo and Bean, 1994; Martina and Jonas, 1997). In the context of the shallow interspike troughs, it is interesting that spontaneous firing was maintained despite a low availability of TTX-sensitive channels before each action potential. Moderate synaptic inhibition that hyperpolarizes the cell therefore may recruit a significant number of sodium channels. Such increases in sodium channel availability may contribute to the tendency to fire during small, steady hyperpolarizations as well as to participate in the rebound excitation that has been observed in these neurons.

Potassium currents

Nearly all of the outward current evoked with action potential waveforms was blocked by 1 mM TEA. This high TEA sensitivity suggests that the calcium-dependent and -independent components arise from the slo (BK) and the KV3 family (Coetzee et al., 1999). These data add cerebellar nuclear cells to the class of neurons in

which fast repolarization of action potentials is driven by KV3 channels (Rudy et al., 1999). *In situ* hybridization studies indicate high expression of KV3.1 and KV3.3, some KV3.2, but no KV3.4 in cerebellar nuclear cells. Consistent with our recordings, these subunits predict high-threshold, noninactivating, fast delayed rectifier-like currents (Weiser et al., 1994, 1995).

Other currents

In cerebellar nuclear neurons in slices, burst firing appears to depend on low-threshold calcium currents and I_h and appears to be regulated by SK currents (Aizenman and Linden, 1999). In isolated cells, although calcium currents may produce some interspike depolarization, they appear to be balanced quickly or overwhelmed by calcium-activated potassium currents. In intact preparations, the contribution of calcium currents to maintaining spontaneous firing is likely to vary with several factors, including channel density, temperature, and recent firing history.

Isolated neurons did not tend to fire bursts of action potentials either after hyperpolarizing current injection or during pharmacological blockade of SK channels. We do not think that these results are primarily a consequence of enzymatic cleavage of the relevant channels. Calcium currents do not appear particularly sensitive to enzymatic cleavage (Mintz and Bean, 1992; Boland et al., 1994; McDonough and Bean, 1998), and several hundred picoamps were present in our isolated cells (I. M. Raman, unpublished data). Similarly, SK currents are retained in papain-dissociated hair cells (Tucker and Fettiplace, 1996), and, in our hands, BMI consistently modified the interspike waveform. In fact, isolated cerebellar nuclear neurons responded to SK channel blockade much like vestibular neurons in slices (du Lac, 1996). Finally, although trypsin can cleave I_h (Budde et al., 1994), our control experiments with papain-dissociated cells of the ventral cochlear nucleus suggest that I_h can withstand our dissociation procedure.

Because of these results, we favor the idea that the bursting depends on channels that have a preferred or enhanced dendritic expression and that therefore are lost or reduced in isolated cells. Specifically, imaging studies of cerebellar nuclear neurons suggest a higher density of calcium channels in dendrites (Muri and Knöpfel, 1994). Electrophysiological studies report larger rebound depolarizations with synaptic IPSPs than with somatic hyperpolarizing currents, suggestive of dendritic expression of currents such as I_h (Aizenman and Linden, 1999). Precedent for restricted dendritic localization of SK channels comes from CA1 hippocampal neurons (Bekkers, 2000).

Physiological implications

The specific properties of the intrinsic currents are likely to determine any responses of the neuron to synaptic stimulation (Llinás, 1988; Stuart and Häusser, 1998). Because Purkinje cells fire spontaneously at high rates *in vivo*, cerebellar nuclear neurons must experience a continual inhibitory drive. The tonic cation current may counteract this inhibition in part, promoting the spontaneous firing observed *in vivo*. When Purkinje cells are excited synaptically to fire above their spontaneous rates, postsynaptic inhibition presumably increases, and the resulting shunt and/or hyperpolarization may slow or suspend the firing of cerebellar nuclear neurons (Jahnsen, 1986b; Mougnot and Gähwiler, 1995; Gauck and Jaeger, 2000). Once Purkinje cell activity returns to the spontaneous level, however, the tonic cation current, along with TTX-sensitive sodium currents that recovered during inhibition or voltage-gated calcium currents, may participate in restoring a regular pattern of firing.

REFERENCES

- Aizenman CD, Linden DJ (1999) Regulation of the rebound depolarization and spontaneous firing patterns of deep nuclear neurons in slices of rat cerebellum. *J Neurophysiol* 82:1697–1709.
- Aizenman CD, Linden DJ (2000) Rapid, synaptically driven increases in the intrinsic excitability of cerebellar deep nuclear neurons. *Nat Neurosci* 3:109–111.
- Alzheimer C, Schwandt PC, Crill WE (1993) Modal gating of Na^+ channels as a mechanism of persistent Na^+ current in pyramidal neurons from rat and cat sensorimotor cortex. *J Neurosci* 13:660–673.

- Bayliss DA, Li Y-W, Talley EM (1997) Effects of serotonin on caudal raphe neurons: activation of an inwardly rectifying potassium conductance. *J Neurophysiol* 77:1349–1361.
- Bekkers JM (2000) Distribution of slow AHP channels on hippocampal CA1 pyramidal neurons. *J Neurophysiol* 83:1756–1759.
- Benos DJ, Stanton BA (1999) Functional domains within the degenerin/epithelial sodium channel (Deg/ENaC) superfamily of ion channels. *J Physiol (Lond)* 520:631–644.
- Bentivoglio M, Kuypers HGJM (1982) Divergent axon collaterals from rat cerebellar nuclei to diencephalon, mesencephalon, medulla oblongata, and cervical cord. *Exp Brain Res* 46:339–356.
- Bevan MD, Wilson CJ (1999) Mechanisms underlying spontaneous oscillation and rhythmic firing in rat subthalamic neurons. *J Neurosci* 19:7617–7628.
- Boland LM, Morrill JA, Bean BP (1994) ω -Conotoxin block of N-type calcium channels in frog and rat sympathetic neurons. *J Neurosci* 14:5011–5027.
- Budde T, White J, Kay AR (1994) Hyperpolarization-activated Na^+/K^+ current (I_h) in neocortical neurons is blocked by external proteolysis and internal TEA. *J Neurophysiol* 72:2737–2742.
- Canessa CM, Schild L, Buell G, Thorens B, Gautschi I, Horisberger J-D, Rossier BC (1994) Amiloride-sensitive epithelial Na^+ channel is made of three homologous subunits. *Nature* 367:463–467.
- Cant NB, Morest DK (1979) The bushy cells of the anteroventral cochlear nucleus of the cat. A study with the electron microscope. *Neuroscience* 4:1925–1945.
- Cepeda C, Chandler SH, Shumate LW, Levine MS (1995) Persistent Na^+ conductance in medium-sized neostriatal neurons: characterization using infrared video microscopy and whole-cell patch-clamp recordings. *J Neurophysiol* 74:1343–1348.
- Chan-Palay V (1977) Cerebellar dentate nucleus. Organization, cytology, and transmitters. Springer: Berlin.
- Coetzee WA, Amarillo Y, Chiu J, Chow A, Lau D, McCormack T, Moreno H, Nadal MS, Ozaita A, Pountney D, Saganich M, Vega-Saenz de Miera E, Rudy B (1999) Molecular diversity of K^+ channels. *Ann NY Acad Sci* 868:233–285.
- Crill WE (1996) Persistent sodium current in mammalian central neurons. *Annu Rev Physiol* 58:349–362.
- Czubayko U, Schwarz C, Sultan F (1998) Rat cerebellar nuclei neurons exhibit slow cyclic firing patterns *in vitro*. *Soc Neurosci Abstr* 24:666.
- Doan TN, Kunze DL (1999) Contribution of the hyperpolarization-activated current to the resting membrane potential of rat nodose sensory neurons. *J Physiol (Lond)* 514:125–138.
- du Lac S (1996) Candidate cellular mechanisms of vestibulo-ocular reflex plasticity. *Ann NY Acad Sci* 781:489–498.
- du Lac S, Lisberger SG (1995) Membrane and firing properties of avian medial vestibular nucleus neurons *in vitro*. *J Comp Physiol [A]* 176:641–651.
- Feigenspan A, Gustincich S, Bean BP, Raviola E (1998) Spontaneous activity of solitary dopaminergic cells of the retina. *J Neurosci* 18:6776–6789.
- Forsythe ID, Redman SJ (1988) The dependence of motoneuron membrane potential on extracellular ion concentrations studied in isolated rat spinal cord. *J Physiol (Lond)* 404:83–99.
- Fredette BJ, Mugnaini E (1991) The GABAergic cerebello-olivary projection in the rat. *Anat Embryol (Berl)* 184:225–243.
- French CR, Sah P, Buckett KJ, Gage PW (1990) A voltage-dependent persistent sodium current in mammalian hippocampal neurons. *J Gen Physiol* 95:1139–1157.
- García-Añoveros J, Derfler B, Neville-Golden J, Hyman BT, Coery DP (1997) BNaC1 and BNaC2 constitute a new family of human neuronal sodium channels related to degenerins and epithelial sodium channels. *Proc Natl Acad Sci USA* 94:1458–1464.
- Gauk V, Jaeger D (2000) The control of rate and timing of spikes in the deep cerebellar nuclei by inhibition. *J Neurosci* 20:3006–3016.
- Ghamari-Langroudi M, Bourque CW (2000) Excitatory role of hyperpolarization-activated inward current in phasic and tonic firing of rat supraoptic neurons. *J Neurosci* 20:4855–4863.
- Gonzalo-Ruiz A, Leichnetz GR, Smith DJ (1988) Origin of cerebellar projections to the region of oculomotor complex, medial pontine reticular formation, and superior colliculus in new world monkeys: a retrograde horseradish peroxidase study. *J Comp Neurol* 268:508–526.
- Grace AA, Onn S-P (1989) Morphology and electrophysiological properties of immunocytochemically identified rat dopamine neurons recorded *in vitro*. *J Neurosci* 9:3463–3481.
- Guérineau NC, Bossu J-L, Gähwiler BH, Gerber U (1995) Activation of a nonselective cationic conductance by metabotropic glutamatergic and muscarinic agonists in CA3 pyramidal neurons of the rat hippocampus. *J Neurosci* 15:4395–4407.
- Hagiwara N, Irisawa H, Kasanuki H, Hosoda S (1992) Background current in sino-atrial node cells of the rabbit heart. *J Physiol (Lond)* 448:53–72.
- Hasuo H, Phelan KD, Twery MJ, Gallagher JP (1990) A calcium-dependent slow afterdepolarization recorded in rat dorsolateral septal nucleus neurons *in vitro*. *J Neurophysiol* 64:1838–1846.
- Häusser M, Clark BA (1997) Tonic synaptic inhibition modulates neuronal output pattern and spatiotemporal synaptic integration. *Neuron* 19:665–678.
- Hodgkin AL, Huxley AF (1952) A quantitative description of membrane current and its application to conduction and excitation in nerve. *J Physiol (Lond)* 117:500–544.
- Ito M, Yoshida M, Obata K, Kawai N, Udo M (1970) Inhibitory control of intracerebellar nuclei by the Purkinje cell axons. *Exp Brain Res* 10:64–80.
- Jacob R, Lieberman M, Liu S (1987) Electrogenic sodium-calcium exchange in cultured embryonic chick heart cells. *J Physiol (Lond)* 387:567–588.
- Jahnsen H (1986a) Electrophysiological characteristics of neurones in the guinea pig deep cerebellar nuclei *in vitro*. *J Physiol (Lond)* 372:129–147.
- Jahnsen H (1986b) Extracellular activation and membrane conductances of neurones in the guinea pig deep cerebellar nuclei *in vitro*. *J Physiol (Lond)* 372:149–168.
- Jones S (1989) On the resting potential of isolated frog sympathetic neurons. *Neuron* 3:153–161.
- Kay AR, Sugimori M, Llinás R (1998) Kinetic and stochastic properties of a persistent sodium current in mature guinea pig cerebellar Purkinje cells. *J Neurophysiol* 80:1167–1179.
- Khawaled R, Bruening-Wright A, Adelman JP, Maylie J (1999) Bicuculline block of small-conductance calcium-activated potassium channels. *Pflügers Arch* 438:314–321.
- Kuo C-C, Bean BP (1994) Na^+ channels must deactivate to recover from inactivation. *Neuron* 12:819–829.
- Lamas JA (1998) A hyperpolarization-activated cation current (I_h) contributes to resting membrane potential in rat superior cervical sympathetic neurones. *Pflügers Arch* 436:429–435.
- Llinás R (1988) The intrinsic electrophysiological properties of mammalian central neurons: insights into central nervous system function. *Science* 242:1654–1664.
- Llinás R, Mühlethaler M (1988) Electrophysiology of guinea pig cerebellar nuclear cells in the *in vitro* brainstem-cerebellar preparation. *J Physiol (Lond)* 404:241–258.
- Llinás R, Sugimori M (1980) Electrophysiological properties of *in vitro* Purkinje cell somata in mammalian cerebellar slices. *J Physiol (Lond)* 305:171–195.
- Llinás RR, Sugimori M, Simon SM (1982) Transmission by presynaptic spike-like depolarization in the squid giant synapse. *Proc Natl Acad Sci USA* 79:2415–2419.
- Lüthi A, McCormick D (1999) Modulation of a pacemaker current through Ca^{2+} -induced stimulation of cAMP production. *Nat Neurosci* 2:634–641.
- Magee JC (1998) Dendritic hyperpolarization-activated currents modify the integrative properties of hippocampal CA1 pyramidal neurons. *J Neurosci* 18:7613–7624.
- Magistretti J, Ragsdale DS, Alonso A (1999a) High conductance sustained single-channel activity responsible for the low-threshold persistent Na^+ current in entorhinal cortex neurons. *J Neurosci* 19:7334–7341.
- Magistretti J, Ragsdale DS, Alonso A (1999b) Direct demonstration of persistent Na^+ channel activity in dendritic processes of mammalian cortical neurones. *J Physiol (Lond)* 521:629–636.
- Manabe K, Takano M, Noma A (1995) Non-selective cation current of guinea-pig endocardial endothelial cells. *J Physiol (Lond)* 487:407–419.
- Marrion NV (1997) Control of M-current. *Annu Rev Physiol* 59:483–504.
- Martina M, Jonas P (1997) Functional differences in Na^+ channel gating between fast-spiking interneurons and principal neurones of rat hippocampus. *J Physiol (Lond)* 505:593–603.
- Mayer ML, Westbrook GL (1983) A voltage-clamp analysis of inward (anomalous) rectification in mouse spinal ganglion sensory neurones. *J Physiol (Lond)* 431:291–318.
- McCobb DP, Beam KG (1991) Action potential waveform voltage-clamp commands reveal striking differences in calcium entry via low- and high-voltage-activated calcium channels. *Neuron* 7:119–127.
- McCormick DA, Pape H-C (1990) Properties of a hyperpolarization-activated cation current and its role in rhythmic oscillation in thalamic relay neurones. *J Physiol (Lond)* 431:291–318.
- McDevitt CJ, Ebner TJ, Bloedel JR (1987) Relationships between simultaneously recorded Purkinje cells and nuclear neurons. *Brain Res* 425:1–13.
- McDonough SI, Bean BP (1998) Mibefradil inhibition of T-type calcium channels in cerebellar Purkinje neurons. *Mol Pharmacol* 54:1080–1087.
- McQuiston AR, Madison DV (1999a) Muscarinic receptor activity has multiple effects on the resting membrane potentials of CA1 hippocampal neurons. *J Neurosci* 19:5693–5702.
- McQuiston AR, Madison DV (1999b) Muscarinic receptor activity induces an afterdepolarization in a subpopulation of hippocampal CA1 neurons. *J Neurosci* 19:5703–5710.
- Millar JA, Barratt L, Southan AP, Page K, Fyfe REW, Robertson B, Mathie A (2000) A functional role for the two-pore domain potassium channel TASK-1 in cerebellar granule neurons. *Proc Natl Acad Sci USA* 97:3614–3618.
- Mintz IM, Bean BP (1992) GABA_B receptor inhibition of P-type Ca^{2+} channels in central neurons. *Neuron* 10:889–898.
- Mouginot D, Gähwiler BH (1995) Characterization of synaptic connec-

- tions between cortex and deep nuclei of the rat cerebellum *in vitro*. *Neuroscience* 64:699–712.
- Muri R, Knöpfel T (1994) Activity-induced elevations of intracellular calcium concentration in neurons of the deep cerebellar nuclei. *J Neurophysiol* 71:420–428.
- Nam SC, Hockberger PE (1997) Analysis of spontaneous electrical activity in cerebellar Purkinje cells acutely isolated from postnatal rats. *J Neurobiol* 33:18–32.
- Nelson BJ, Mugnaini E (1989) Origins of GABAergic inputs to the inferior olive. In: *The olivocerebellar system in motor control* (Strata P, ed), pp 86–107. Berlin: Springer.
- Oertel D (1983) Synaptic responses and electrical properties of cells in brain slices of the mouse anteroventral cochlear nucleus. *J Neurosci* 3:2043–2053.
- Patlak JB, Ortiz M (1986) Two modes of gating during late Na⁺ channel currents in frog sartorius muscle. *J Gen Physiol* 87:305–326.
- Pennartz CM, Bierlaagh MA, Geurtsen AMS (1997) Cellular mechanisms underlying spontaneous firing in rat suprachiasmatic nucleus: involvement of a slowly inactivating component of sodium current. *J Neurophysiol* 78:1811–1825.
- Raman IM, Bean BP (1997) Resurgent sodium current and action potential formation in dissociated cerebellar Purkinje neurons. *J Neurosci* 17:4517–4526.
- Raman IM, Bean BP (1999) Ionic currents underlying spontaneous action potentials in isolated cerebellar Purkinje neurons. *J Neurosci* 19:1663–1674.
- Raman IM, Trussell LO (1992) The kinetics of the response to glutamate and kainate in neurons of the avian cochlear nucleus. *Neuron* 9:173–186.
- Raman IM, Sprunger LK, Meisler MH, Bean BP (1997) Altered sub-threshold sodium currents and disrupted firing patterns in Purkinje neurons of *Scn8a* mutant mice. *Neuron* 19:881–891.
- Reimann F, Ashcroft FM (1999) Inwardly rectifying potassium channels. *Curr Opin Cell Biol* 11:503–508.
- Rudy B, Chow A, Lau D, Amarillo Y, Ozaita A, Saganich M, Moreno H, Nadal MS, Hernandez-Pineda R, Hernandez-Cruz A, Erisir A, Leonard C, Vega-Saenz de Miera E (1999) Contributions of Kv3 channels to neuronal excitability. *Ann NY Acad Sci* 868:304–343.
- Ruigrok TJH (1997) Cerebellar nuclei: the olivary connection. *Prog Brain Res* 114:167–192.
- Sah P, Gibb AJ, Gage PW (1988) The sodium current underlying action potentials in guinea pig hippocampal CA1 neurons. *J Gen Physiol* 91:373–398.
- Santoro B, Chen S, Lüthi A, Pavlidis P, Shumyatsky GP, Tibbs GR, Siegelbaum SA (2000) Molecular and functional heterogeneity of hyperpolarization-activated pacemaker channels in the mouse CNS. *J Neurosci* 20:5264–5275.
- Sastry BR, Morishita W, Yop S, Shew T (1997) GABAergic transmission in deep cerebellar nuclei. *Prog Neurobiol* 53:259–271.
- Shinoda Y, Izawa Y, Sugiuchi Y, Futami T (1997) Functional significance of excitatory projections from the precerebellar nuclei to interpositus and dentate nucleus neurons for mediating motor, premotor, and parietal cortical inputs. *Prog Brain Res* 114:193–207.
- Spruston N, Johnston D (1992) Perforated patch-clamp analysis of the passive membrane properties of three classes of hippocampal neurons. *J Neurophysiol* 67:508–529.
- Stafstrom CE, Schwindt PC, Chubb MC, Crill WE (1985) Properties of persistent sodium conductance and calcium conductance of layer V neurons from cat sensorimotor cortex *in vitro*. *J Neurophysiol* 53:153–170.
- Stuart G, Häusser M (1998) Shunting of EPSPs by action potentials. *Soc Neurosci Abstr* 24:1810.
- Swandulla D, Lux HD (1985) Activation of a nonspecific cation conductance by intracellular Ca²⁺ elevation in bursting pacemaker neurons of *Helix pomatia*. *J Neurophysiol* 54:1430–1443.
- Tabata T, Ishida AT (1996) Transient and sustained depolarization of retinal ganglion cells by I_h. *J Neurophysiol* 75:1932–1943.
- Teune TM, van der Burg J, Ruigrok TJH (1995) Cerebellar projections to the red nucleus and inferior olive originate from separate populations of neurons in the rat: a nonfluorescent double labeling study. *Brain Res* 673:313–319.
- Teune TM, van der Burg J, DeZeeuw CI, Voogd J, Ruigrok TJH (1998) Single Purkinje cell can innervate multiple classes of projection neurons in the cerebellar nuclei of the rat: a light microscopic and ultrastructural triple-tracer study in the rat. *J Comp Neurol* 392:164–178.
- Thach WT (1968) Discharge of cerebellar neurons during rapidly alternating arm movements in the monkey. *J Neurophysiol* 31:785–797.
- Trotier D, Døving KB (1996) Direct influence of the sodium pump on the membrane potential of vomeronasal chemoreceptor neurones in frog. *J Physiol (Lond)* 1996 490:611–621.
- Tucker TR, Fettiplace R (1996) Monitoring calcium in turtle hair cells with a calcium-activated potassium channel. *J Physiol (Lond)* 494:613–626.
- Uteshev VV, Stevens DR, Haas HL (1995) A persistent sodium current in acutely isolated histaminergic neurons from rat hypothalamus. *Neuroscience* 66:143–149.
- Weiser M, Vega-Saenz de Miera E, Kentros C, Moreno H, Franzen L, Hillman D, Baker H, Rudy B (1994) Differential expression of Shaw-related K⁺ channels in the rat central nervous system. *J Neurosci* 14:949–972.
- Weiser M, Bueno E, Sekirnjak C, Martone ME, Baker H, Hillman D, Chen S, Thornhill W, Ellisman M, Rudy B (1995) The potassium channel subunit KV3.1b is localized to somatic and axonal membranes of specific populations of CNS neurons. *J Neurosci* 15:4298–4314.
- Williams JT, North RA, Shefner SA, Nishi S, Egan TM (1984) Membrane properties of rat locus coeruleus neurones. *Neuroscience* 13:137–156.
- Williams SR, Stuart GJ (2000) Site independence of EPSP time course is mediated by dendritic I_h in neocortical pyramidal neurons. *J Neurophysiol* 83:3177–3182.
- Wilson GF, Richardson FC, Fisher TE, Olivera BM, Kaczmarek LK (1996) Identification and characterization of a Ca²⁺-sensitive nonspecific cation channel underlying prolonged repetitive firing in *Aplysia* neurons. *J Neurosci* 16:3661–3671.
- Yellen G (1982) Single Ca²⁺-activated nonselective cation channels in neuroblastoma. *Nature* 296:357–359.
- Yung WH, Häusser MA, Jack JJB (1991) Electrophysiology of dopaminergic and non-dopaminergic neurones of the guinea pig substantia nigra pars compacta *in vitro*. *J Physiol (Lond)* 436:643–667.
- Zhang YH, Youm JB, Sung HK, Lee SH, Ryu SY, Ho WK, Earm YE (2000) Stretch-activated and background non-selective cation channels in rat atrial myocytes. *J Physiol (Lond)* 523:607–619.